In situ community dynamics influences the temperature- and light- dependent succession of seasonal phytoplankton

Margot Tragin, Stefan Lambert, Jean-Claude Lozano, François-Yves Bouget

1   **In situ community dynamics influences the temperature- and light- dependent**

2   **succession of seasonal phytoplankton**

3   Margot Tragin[1], Stefan Lambert[1], Jean-Claude Lozano[1], François-Yves Bouget[1,2]

4   [1] Sorbonne Université, CNRS, UMR7621, Laboratory of Microbial Oceanography, Observatoire

5   Océanologique, Avenue Pierre Fabre, 66650 Banyuls sur mer, France

6   [2] Corresponding author: fy.bouget@obs-banyuls.fr

7

8   **Compliance with ethical standards**

9   The authors declare that they have no conflict of interest.

10

Abstract

11

12   Temperature and light play a crucial role in regulating phytoplankton blooms in the

13   Ocean. To assess the importance of these two parameters experimentally, microcosms were

14   conducted on seven picoplankton communities (<3 µm) sampled in December, March, June and

15   September 2015 and 2016 in the North Western Mediterranean Sea. Each community was

16   exposed to 4 realistic seasonal conditions (December, March, June and September).

17   Metabarcoding was used to investigate the eukaryotic diversity in the 56 microcosms

18   experiments in parallel to high-frequency monitoring of environmental diversity in the sea. The

19   three major lineages identified were the Stramenopiles, Alveolata and Archaeplastida. Overall,

20   the five-day incubations were not sufficient to reshape the initial microbial communities

21   completely. The microcosm outcome was strongly influenced by the dynamics of phytoplankton

22   starting communities. In pre-bloom conditions, phytoplanktonic species were the most sensitive

23   to temperature and light conditions. During a bloom, species belonging to diatoms or

24   Chlorodendrophyceae usually did not respond to light and temperature in microcosms and

25   continued to bloom independently of the applied seasonal condition. Together, these results

26   suggest that light and temperature seasonal conditions play a crucial role in regulating

27   phytoplankton dynamics in pre-bloom conditions and biotic interactions may be preponderant in

28   bloom and post-bloom conditions.

29   **<u>Keywords</u>**

Introduction

As soon as marine planktonic life was discovered in the late XIX century, several studies reported phenology of plankton abundance [1]. The organisms size, whose seasonal pattern were described, evolved together with improvements of detection methods, from light microscopy to molecular techniques. The annual temporality of zooplankton such as copepods and large size phytoplankton such as diatoms and dinoflagellates has been studied for over a century in Northern Mediterranean Sea waters [1–5]. Later, small size picophytoplankton (cell size < 3 μm), such as the green picoalga *Micromonas* sp. were found to seasonally grow also in the Mediterranean sea [6, 7]. In the nineties, extensive microscopy-based taxonomic survey reported that photosynthetic dinoflagellates and diatoms had strong seasonal patterns in NW Mediterranean Sea coastal waters and described sequential phytoplankton spring blooms in the bay of Villefranche sur Mer (France): diatoms blooming in late spring and autumn while dinoflagellates being more abundant in summer [8]. More recently, the development of molecular analyses and high throughput sequencing enabled the tracking of all planktonic organisms' temporal distribution, including the picoplankton [9]. In recent years, the development of molecular analyses and high throughput sequencing allowed the extensive monitoring at an unprecedented taxonomic level, the temporal succession of all planktonic organisms including the smallest protists (i.e., picoplankton cell size < 3 μm).

A time series metabarcoding approach conducted in the bay of Banyuls sur Mer (North Western Mediterranean Sea, France) over seven years revealed a strong temporal factor driving the biogeography of dinoflagellates and pico-sized green alga (Chlorophyta) belonging to the Mamiellophyceae class (*Bathycoccus* and *Micromonas*) [9, 10]. A quarter of photosynthetic reads were commonly assigned to Chlorophyta using 18S rRNA metabarcoding, describing pan-oceanic datasets [11]. The beginning of bloom events appears to be predictable by mathematical models that combine both nutrients, temperature and light parameters with hydrodynamics

57   factors [12]. *In situ* high frequency sampling also unveiled the importance of daily variations in

58   wind or rain on microbial community structures [13]. In addition to meteorological events,

59   hydrographic modifications of environmental factors, which are thought to drive the seasonality

60   of plankton, biotic interactions such as parasitism [14] were assumed to be influencing the end

61   of blooming dynamics in marine waters [15].

62   Microcosm experiments have been used for decades to address a large panel of questions

63   experimentally. Methodological approaches are not standardized regarding parameters such as

64   temperature, nutrients or pH and targeted organisms (i.e., prokaryotes, pico- or nanoeukaryotes,

65   phototrophs or heterotrophs). The duration of incubations commonly varied from several hours

66   [16], to days [17], or even weeks [18, 19]. In the bay of Banyuls, two parameters, temperature

67   and daylight, account for half of eukaryotic phytoplankton variability in one of the most

68   extended metabarcoding time series (7 years) reported to date [9]. In this study, we combine

69   microcosms and time series approaches in the bay of Banyuls to investigate the resilience of

70   protists seasonality to light and temperature parameters, set up to mimic realistic seasonal

71   conditions of daylight (photoperiod, intensity) and temperature. Over five days, incubations

72   were performed that matched the gap between two successive samples in our high frequency

73   (159 samples between 2015-2017) time series. These experiments aim at addressing the

74   following questions: (1) How do abrupt changes in light and temperature alter picoeukaryotic

75   communities? (2) How quickly can we change the protist communities from the initial season

76   towards protist communities representative of the mimicked season? (3) How does the starting

77   community dynamics influence microcosm outcome?

Material and Methods

Microcosms experiments

Five liters of seawater were sampled at SOLA buoy in the bay of Banyuls (42°31′N, 03°11′E, France). Three µm filtration was used to remove large grazers and nanoplanktonic predators such as ciliates and flagellates since they can induce strong bias in small volume microcosms. Four times 400 ml pre-filtered seawater were incubated in 500 ml aerated culture flasks (Sarstedt) in homemade incubators equipped with white wide spectrum LEDs mimicking realistic light conditions (photoperiod and light intensity, Fig. 1). For each date, microcosms were conducted in triplicates. In addition, the complete set of 84 incubations (7 dates x 4 conditions x triplicates) was done twice with and without nitrate and phosphate enrichments (NP). Five µM of $NaNO_3$ (SIGMA Aldrich) and 0.2 µM of Na_2HPO_4 (SIGMA Aldrich) were added in NP enriched microcosms, which corresponded to maximal annual concentrations measured in the Banyuls Bay [9]. The planktonic abundance in the 56 microcosms (x3) was followed daily using an ACCURI C6 flow cytometer (BD Biosciences) as previously described [9]. After five days of incubation, triplicates were pooled, filtered on 0.22 µm Sterivex (Merck-Millipore) and stored at -80 °C prior to DNA extraction.

DNA extraction, amplification and sequencing

DNA extracted from SOLA high-frequency time series and microcosm experiments were amplified and sequenced. DNA extractions were performed following the same protocol as Hugoni *et al* [20] and Lambert *et al* [9]. The V4 region of the 18S rRNA gene was amplified using the TAReuk primers 5'-CCAGCASCYGCGGTAATTCC (forward) and 5'-ACTTTCGTTCTTGATYRATGA (reverse) modified from Stoeck *et al* [21]. Then, paired-end Illumina sequencing Miseq (2x250 base pairs) was performed by the Genotoul platform

101   (Toulouse, France). SOLA high-frequency time series metabarcoding datasets are available on

102   NCBI under accession number PRJNA579489.

103   **Bioinformatics treatment of metabarcoding data**

104   SOLA high-frequency time series and microcosms metabarcoding datasets were

105   analyzed separately but using identical DADA2 bioinformatics pipeline version 1.6 [22]

106   implemented in R v 3.6.1. The parameters were set as: trimLeft=c(20, 21), maxN=0,

107   maxEE=c(2,2), truncQ=2 and truncLen=c(250,250) respectively c(280,230) to analyze the time

108   series and the microcosms data. To allow comparison between the two datasets (e.g., in terms of

109   shared Amplicon Sequence Variants (ASVs)), SOLA and microcosms ASVs and count tables

110   were pulled together and re-processed under Mothur pipeline v1.35.1 [23] after keeping a single

111   copy of each ASV using the *unique.seqs()* function, ASVs were taxonomically re-classified

112   using the Protist Ribosomal Reference Database v4.11.1 [PR^2, 24, https://pr2-database.org/] in

113   which several protists groups were recently curated such as Chlorophyta [25], Haptophyta [26]

114   and dinoflagellates [27].

115   **Statistics and data visualization**

116   Statistics and graphics were performed using R software version 3.6.1. Calculation of

117   Simpson diversity index [28] and richness (Sup. Data 1), Bray-Curtis dissimilarity matrix used

118   for Non-parametric Multi-Dimensional Scaling (NMDS, Sup. Data 2) and SIMPER [similarity

119   percentage analysis, 29] test were performed using the *vegan* v. 2.5.6. R packages. Common R

120   packages such as *Treemap* (e. g. used for Sup. Data 4) or *Hmisc* to plot standard deviation were

121   also used to produce figures. All R scripts were formatted using the *Rmd* R packages and are

122   available in supplementary data (Sup. Data 1to Sup. Data 5).

123

Results

Flow cytometry analysis of microcosms

Microcosm incubation experiments were performed in parallel to the high-frequency time series at SOLA buoy in the bay of Banyuls (42°31′N, 03°11′E, France) between January 2015 and March 2017 [30]. Microbial community from SOLA were sampled and filtered at seven dates (between spring 2015 and autumn 2016) corresponding to each of the four seasons (Supplementary table 1). Samples filtered on 3 µm were exposed in triplicates to realistic light conditions (photoperiod and light intensity) and temperature of the four seasons at the Banyuls latitude (Fig.1). After five days, photosynthetic cell abundance ranged from 290 (December 2016) to 32 000 cells.ml^{-1} (March 2015) with an average value of 6 300 cells.ml^{-1} in microcosms lacking nutrients supplementation (Supplementary Fig. 1 A) and from 540 cells.ml^{-1} (June 2015) to 100 700 cells.ml^{-1} (March 2015) with an average value of 11 730 cells.ml^{-1} in NP enriched microcosms (Supplementary Fig. 1 B). Overall, the triplicate showed the same pattern of growth even though deviations were occasionally observed (e.g., for sample 3-3 at day 5). Different patterns of picophytoplankton growth were observed between microcosms. While cell growth was observed in microcosms 1 and 7, an increase in cell number occurred only at day 5 for Microcosms 2 and 5 and a decrease of picophytoplankton cells in all triplicates was observed over the time course of microcosm 4.

Major eukaryotic groups recovered by metabarcoding

Microcosms and environmental samples metabarcodes represented around 2 million reads, which were distributed into 2395 ASVs (Supplementary Table 2). Only ASVs represented by more than ten identical reads were taken into account. ASVs size ranged from 11 to 271 707 reads (ASV assigned to Syndiniales) with an average size of 62 reads. ASVs were assigned to the nine eukaryotic supergroups present in the PR² database taxonomy [24], yet 373 ASVs were unassigned at this taxonomic level. Stramenopiles, Alveolata, Archaeplastida and Rhizaria

149   supergroups were the four most represented in microcosm ASVs (Fig. 2 A) while Alveolata,

150   Stramenopiles, Archaeplastida and Hacrobia were the main supergroups recovered from the

151   SOLA environmental time series ASVs (Fig. 2 B). Reproducible seasonal patterns of ASV

152   abundance were observed for both photosynthetic and heterotrophic (e.g. Opisthokonta and

153   Alveolata) eukaryotes (Supplementary Fig. 2 A). Photosynthetic eukaryotes were detected

154   primarily between late autumn and early Spring each year (Supplementary Fig. 2 B).

155   Stramenopiles were represented by 503 559 reads split into 671 ASVs, in which 272 791

156   reads (373 ASVs) were assigned to the photosynthetic Ochrophyta division (Fig. 2). In this

157   division, reads were also assigned to the environmental clades MAST (marine Stramenopiles,

158   153 204 reads, 156 ASVs) and MOCH (marine Ochrophyta, 105 492 reads, 28 ASVs, [31]). In

159   SOLA, Diatoms (Bacillaryophyta) drove Ochrophyta temporal dynamics, especially in late

160   autumn, winter and early spring (Supplementary Fig. 3).

161   Alveolata were represented by 436 920 reads (assigned to 757 ASVs), in which most were

162   assigned to dinoflagellates (422 358 reads, 628 ASVs). In SOLA, Alveolata reads were assigned

163   to Dinophyceae, Syndiniales (especially the Dino-group I clade 1) and to a lower extent to

164   grazers such as the Spirotricheae Ciliophora (Supplementary Fig. 2). For example, in sample 2-

165   1, 85% of Alveolata reads corresponded to Syndiniales, which have been described as parasites

166   of protists [32, 33].

167   Archaeplastida supergroup was represented by 12 ,612 assigned reads (137 ASVs),

168   including Chlorophyta taxa (119 200 reads, 104 ASVs). In SOLA, Chlorophyta was the second

169   major photosynthetic group (Dinoflagellates excluded). Dinoflagellates are commonly excluded

170   from photosynthetic groups when using metabarcoding because only half of the species are

171   photosynthetic. Moreover, Alveolata have large repeated genomes with numerous copies of the

172   18S rRNA gene, that can bias reads relative counts [34–36]. Remarkably, even with a limited

173   number of 18S rRNA genes copies per genome, Chlorophyta numbers of reads were as high as

174 those of Syndiniales (Supplementary Fig. 2 B) and Ochrophyta (Supplementary Fig. 2 C) and

175 even higher in winters 2015-16. The succession of Chlorophyta classes is detailed below.

176

Microcosms ecological patterns

178 The number of ASVs (i.e., richness) ranged from 52 in sample 1-4NP (water sampled in

179 March 2015 and incubated in December artificial conditions with nitrate and phosphate

180 enrichment) to 636 in sample 6-4 (seawater sampled in October 2016 and set in December

181 artificial conditions, Supplementary Table 1). On average, 177 ASVs were recovered per

182 sample. The Simpson diversity index ranged from 0.41 in sample 5-4NP to 0.99, with an

183 average Simpson index of 0.87. During microcosm experiments, the diversity stayed high

184 (between 0.8 and 1) except for June 2016 (Fig. 3), while the richness decreased in microcosm

185 experiments compared to natural samples (Fig. 3). In general, microcosms acted as a filter,

186 which reduced the number of ASVs without unbalancing the proportion of these ASVs in

187 samples except for 4 June sampled microcosms and sample 6-4, which showed a higher richness

188 but the same diversity than its relative natural counterpart samples (6-0 and 6-5). The natural

189 samples 4-5 and 7-5 differed from other natural samples by their low Simpson's diversity index

190 (around 6.5) and low richness (< 100 ASVs, Fig. 3). The four June microcosm (2-1, 5-1, 5-1NP

191 and 5-4NP) showed the lowest Simpson's diversity index in the dataset and a low richness (<

192 100 ASVs, Fig. 3).

193 The representation of all natural and microcosms samples on an NMDS plot revealed that

194 both natural communities and microcosm incubated samples were grouped according to

195 sampling time rather than incubation conditions (Fig. 4). Natural samples clustered together

196 with microcosms in June and October, March 2016 and December 2016 but were clearly

197 separated in March 2015 (1-0 and 1-5) and December 2015 (3-0 and 3-5) indicating that

198 changes in microbial communities had occurred in microcosm 1 and 3. Finally, environmental

199   samples (4-0 and 4-5) as well as (7-0 and 7-5) were well separated revealing that changes in

200   communities had occurred in the field during microcosms. Microcosms incubated with or

201   without nitrate and phosphate (NP) enrichment clustered together, suggesting that the

202   enrichment did not induce major changes in microbial communities. (Procrustean statistic

203   confirmed that microcosms with and without NP enrichment were highly correlated (R^2=0.86,

204   Pvalue=$9.9e^{-5}$). For this reason, only microcosms lacking NP enrichment were kept in the

205   analysis thereafter.

206   Most microcosm samples showed an increase in the relative abundance of Alveolata (e.g.,

207   Syndiniales dino group I clade and in a lesser extent *Gyrodinium* sp.), Opisthokonta

208   (microcosms 1-1 to 1-4, 2-1 to 2-4, 5-2, 5- 3) or Rhizaria (for example in 2-2, 2-3, 5-2, 5-3, 6-2

209   and 6-3 samples) relative contributions (Fig. 4, Supplementary Fig. 2). These three groups were

210   the most represented heterotrophic protists. Concerning photosynthetic groups, several

211   microcosms (such as 4-2, 4-3, 5-2, 5-3, 7-1 and 7-3 samples, Fig. 5) differed from the others by

212   their major contribution of Stramenopiles, which were usually associated to warmer incubations

213   conditions (June and September). The Chlorophyta relative contributions were higher in

214   microcosms sampled in March and June (sample 1-2 to 1-4, 2-4, 5-4, 4-1 and 4-4 for example,

215   Fig. 5).

216   **Chlorophyta**

217   We next focused on Chlorophyta, which provides an interesting case study of seasonal

218   succession with ASVs belonging to this group found all year round in SOLA. In the time series,

219   161 ASVs were assigned to Chlorophyta, among which Mamiellophyceae (41 ASVs) and

220   Chlorodendrophyceae (9 ASVs) dominated the green microalgae community, both showing

221   clear seasonal patterns (Fig. 6 A). Mamiellophyceae represented 100 % of Chlorophyta reads

222   between January and March 2015 and in 2016, and more than 80 % between October and

223   December 2016. Chlorodendrophyceae represented up to 60 % of Chlorophyta reads from April

224   to early September in 2015 and 2016. The number of reads assigned to other Chlorophyta

225   classes and their relative contribution to Chlorophyta was too low to identify clear seasonal

226   patterns. Mamiellophyceae and Chlorodendrophyceae did rarely co-occur in time (Fig. 6 A).

227   Mamiellophyceae reads were recovered mainly in winter and early spring while

228   Chlorodendrophyceae reads followed Mamiellophyceae peaks of abundance from late spring to

229   late summer.

230   In microcosm experiments, the relative contribution of Chlorophyta usually decreased

231   to the benefit of Alveolata or Stramenopiles reads, except in microcosm 1 (March 2015, Fig. 5).

232   SIMPER analyses found between 2 and 4 ASVs assigned to Chlorophyta (e.g., M0005

233   *Bathycoccus*, M0010 *Micromonas* or M0050 Chlorodendrales) involved in the dissimilarity

234   between samples in all incubations except for microcosm 6 (Supplementary Fig. 2). In the

235   microcosm metabarcoding dataset, Chlorophyta reads were mainly assigned to

236   Mamiellophyceae or Chlorodendrophyceae classes, but also to Chloropicophyceae (samples 3-2

237   to 3-4, 4-1 and 4-4) and Trebouxiophyceae (samples 1-1 to 1-4, 4-1 and 4-4, Fig. 6 B).

238   Mamiellophycae dominated both incubated and natural samples in microcosms 3, 4 and 7, while

239   Chlorodendrophyceae dominated both incubated and natural samples in microcosms 2 and 5. In

240   microcosm experiments 1 and 4, the dominant Chlorophyta class switched between natural and

241   incubation samples indicating that incubations profoundly modified the Chlorophyta

242   community. Experiment 1 and 4 (March) showed respectively Chlorodendrophyceae (ASV

243   M0050, Supplementary Table 3) and Chloropicophyceae (ASV M0037, Supplementary Table

244   3) as dominant Chlorophyta class, while Mamiellophyceae dominated natural samples sampled

245   (1-0, 1-5 and 4-0, since very low reads of Chlorophyta were assigned to 4-5, Fig. 6).

246   Moving to the genus taxonomic level, Mamiellophyceae dominant genera in the SOLA

247   time series were *Micromonas* and *Bathycoccus* (Supplementary Fig. 5). Across the three studied

248   winters (2015, 2016 and 2017), *Micromonas* peaks arrived in early winter followed by

249   *Bathycoccus* peaks in late winter or early spring (Supplementary Fig. 4 A). In microcosms, the

250   number of reads assigned to Mamiellophyceae was low in samples from the microcosms 1, 3

251   and 4. Nevertheless, Simper statistic tests unveiled that *Micromonas* (ASVs M0010 and M0046)

252   and *Bathycoccus* (M0005) contributed significantly to the dissimilarities between samples in

253   experiments 1, 3, 4 and 7 (Supplementary Table 3). *Micromonas* reads were recovered in

254   samples 7-1, 7-3 and 7-4, while *Bathycoccus* dominated sample 4-4 (Supplementary Fig. 4 B).

255   Mamiellophyceae (especially *Micromonas*) were usually more abundant under low temperature,

256   i.e. when the applied temperature in microcosms was similar or lower than the environmental

257   temperature (i.e., in conditions 1-March and 4-December the temperature was circa 14°C).

258

259   Discussion

260   Metabarcoding versus flow cytometry

261   Metabarcoding of the 18S rRNA gene V4 region revealed changes in microbial

262   community composiion in response to seasonal conditions of light and temperature in all

263   microcosms. Metabarcoding of 18S rRNA is a non-selective but also non-quantitative method

264   since it depends on the number of 18S rRNA gene copies in protists genomes. Alveolata and to

265   a lesser extent in Stramenopiles supergroups, which have large genomes with numerous copies

266   of 18S rRNA genes, are usually overestimated in metabarcodes datasets [35, 36]. In contrast,

267   Chlorophyta have relatively small genomes and few copies of the 18S rRNA gene (e.g., 3 in

268   *Ostreococcus tauri*) that lead to underestimating their number. Metabarcoding, therefore

269   provides a good picture of the relative contribution of protists in global marine microbial

270   communities [37] as well as of the diversity within specific groups such as diatoms [38] or

271   green microalgae [11] but does not provide information on the impact of cell growth or

272   mortality on community composition. Although less resolutive than metabarcoding, flow

273 cytometry is a quantitative method that captures the daily change of cell numbers in microcosms

274 over five days.

275   Changes in photosynthetic cell numbers, as determined by flow cytometry, were

276 consistent between triplicates in most microcosms, although more variability was occasionally

277 observed as seen in samples 7-2 and 3-3 (Supplementary Fig. 1). Several factors could account

278 for this variability. Though a filtration protocol was used to remove nano-phytoplankton

279 containing predators, some larger-sized grazers of picophytoplankton can sometimes pass

280 through the 3 µm filter and induce disturbances in microcosms.

281   Flow cytometry data showed season dependent growth patterns that could be potentially

282 explained by the initial density of photosynthetic cells in microbial communities. In winter, low

283 photosynthetic cells density allows an exponential growth pattern in each experiment, while in

284 June and March, photosynthetic communities should face both higher competition between

285 microalgae and interactions such as parasitism or grazing, which generally occurs at higher

286 photosynthetic cells density [7, 14].

287 **Effects of five days incubation on microbial communities**

288   The five-day incubations affected the different taxa differently, as illustrated for

289 Hacrobia a division which comprises Cryptophyta and Haptophyta. For example, the

290 contribution of Cryptophyta drastically decreased in all samples of microcosms 1 and 3 (March

291 2015 and December 2015), respectively, while natural samples showed a relatively high

292 contribution of Cryptophyta reads (Fig. 5). In microcosm 6 (October 2016), however, the

293 relative contribution of Haptophyta remains stable between natural communities and

294 microcosms. These observations suggest that, unlike Haptophyta, Cryptophyta from the Banyuls

295 Bay may be too difficult to grow or maintain in microcosms.

296   Stramenopiles was the division that showed the highest differences between

297 microcosms and environmental samples (T5). Its relative contribution showed massive increase

298 in several microcosms (such as 4-2, 4-3, 5-2, 5-3, 3-1, 3-2, 3-3, 7-1, 7-3, 7-4 and experiment 6

299 samples, Fig. 5). This increase in relative contribution should be interpreted in the light of flow

300 cytometry data on day 5. In microcosms 4 (March 2016), we observed a dramatic decrease in

301 photosynthetic cell number (from 10 000 events to 2000), suggesting that the relative increase

302 of Stramenopiles may result from cell mortality in other divisions, such as Archeaplastida. In

303 microcosm 7 (December 2016) in contrast, the global increase in photosynthetic cells observed

304 by flow cytometry suggested that this increase could correspond to diatoms bloom (Ochrophyta,

305 Simper test,Supplementary Table 3). Diatoms occurred in several size fractions [39, 40] and

306 recovering blooms of diatoms in picoeukaryotes microcosms were expected as they are an

307 important phytoplanktonic organism in Mediterranean Sea waters and were already described to

308 follow clear seasonal patterns [41, 42].

309 When Stramenopiles were less abundant, the natural communities and microcosms were

310 often dominated by Alveolata, particularly Syndiniales [which contain known paratisoids, 32,

311 33] were clearly more abundant in microcosms than in environmental samples. In general, the

312 higher relative contribution of heterotrophic protists and putative parasites, such as Syndiniales

313 and *Labyrinthule* in microcosms suggest that the incubation process may enhance infection

314 processes. In addition, the presence of bacterial grazers such as Choenoflagellates, or the ciliate,

315 as *Minoresa minuta* yet [43] evoked that post-bloom conditions were met after five days of

316 incubation days with a decrease of the photosynthetic contribution to the benefit of heterotrophs

317 in several microcosms. The effect of "bottle enclosure" in small volume may be responsible for

318 speeding up biological processes and unbalancing the autotrophic to heterotrophic ratio in

319 microcosms [16, 44].

320 **Effects of light and temperature on microbial community composition in microcosms**

321 It is usually challenging to discriminate between light and temperature effects on

322 microbial communities since these two parameters co-vary in the environment. March and

323   September have similar day length and light conditions among the four seasonal conditions but

324   have an 8°C temperature difference. Comparing microcosms conditions of March and

325   September allows thus, to assess the respective effects of light and temperature. Incubations

326   under these two months' conditions led to dramatic changes in community compositions,

327   highlighting the importance of temperature in shaping microbial communities. In particular,

328   Stramenopiles' relative contribution increased markedly in September warm condition but not in

329   March cold condition as seen in microcosms. Stramenopiles contribution was also high under

330   the June warm condition, confirming the temperature effect on Stramenopiles. Recent

331   microcosm studies have emphasized the putative role of diatoms in a warming ocean, consistent

332   with Stramenopiles exceeding natural relative contribution in the warmest incubated conditions

333   [18]. However, it should be noted that in microcosms 3 and 6, the Stramenopiles contribution

334   was high in a majority of conditions.

335   **Influence of initial communities**

336   Overall, the five-day incubation did not change the protist community enough to switch

337   the incubated community to a community representative of the applied seasonal condition in

338   most microcosms (Fig. 4).. The inter-annual variations between 2015 and 2016 could explain

339   most of the differences seen between microcosms sampled during similar seasons. In general,

340   microcosms and natural samples 2015 and 2016 clustered together (Fig. 4), except for natural

341   samples from microcosms 1 and 3 (March and December 2015). This suggested that winter

342   2015 was different from winter 2016. The environmental parameters, especially temperature

343   and Chl, measured at the SOLA SOMLIT Station were similar between March 2015 and 2016

344   (around 12°C and 0.8-1.7 µg/L). Inter-annual variability was driven mainly by dinoflagellates

345   blooms, which could account for the observed inter-annual differences in March and December

346   between 2015 and 2016 (Supplementary Table 3). Differences between natural samples and

347   microcosms dynamics were also observed in March 2015 (microcosm 1) in which the

348 incubation condition was sufficient to move the march 2015 natural community towards a

349 "2016 like" community. The increase of temperature in 2015 induced a dinoflagellates bloom

350 (e.g. *Gyrodinium* sp.) even though dinoflagellates were not blooming in natural samples. The

351 blooming dynamics allow photosynthetic protists to rapidly dominate communities when

352 environmental conditions became favorable. Blooms occurring in microcosms suggest that

353 microalgae had encountered both favorable environmental conditions and out-competed other

354 protists.

355   The dynamics of natural communities also seem to affect the outcome of microcosms.

356 In microcosms 4 and 5 sampled before a bloom (Supplementary Fig. 2 B, Supplementary Fig. 3)

357 Chrysiophyceae gold microalgae bloomed only in incubation conditions of warm temperature

358 (Fig. 5, Supplementary Table 3). On the contrary, in microcosms 3 (December), 6 (October

359 2016) and 7 (December 2016) sampled at the beginning or during a diatom bloom,

360 Stramenopiles bloomed under all applied seasonal conditions even at a lower temperature (Fig.

361 5, Supplementary Fig. 1). These results lead to the idea of a "community inertia" for blooming

362 species such as diatoms: When the blooming dynamics was already triggered, this dynamics

363 continued independently of the environmental parameters applied. In contrast, under pre-bloom

364 conditions, the environmental parameters strongly influenced the communities in microcosms.

365 **Temporal succession of Chlorophyta**

366   Chlorophyta, in particular Mamiellophyceae, provide an interesting case study since

367 their contribution is major in coastal waters [25, 45]. *Micromonas* and *Bathycoccus* peak in

368 winter in the northern Mediterranean Sea where they can represent more than 50% of

369 picoeukaryotes reads in winter with strong seasonal rhythms [6, 9]. The presence of seasonal

370 Chlorodendrophyceae was only recently confirmed using the V4 region of the 18S rRNA gene

371 metabarcoding technique [10, 11]. Chlorodendrophyceae is an abundant yet poorly documented

372 Chlorophyta class and the major ASVs assigned to Chlorodendrophyceae in SOLA natural

373　samples and microcosms could be assigned only at the order level (Chlorodendrales) and to

374　uncultured organisms (i.e., environmental sequences). SOLA Chlorodendrophyceae seasonal

375　pattern (Fig. 5) was similar to this of *Tetraselmis wettsteinii* [46], a Chlorodendrophyceae

376　species which was shown to form massive green blooms in the Bay of Naples in late spring and

377　summer [47]. Since no reference sequence is available for *T. wettsteinii*, it is not possible to

378　decipher if the abundant Chlorodendrophyceae ASV from the Banyuls Bay corresponds to this

379　species.

380　　　　Interestingly, Mamiellophyceae did not always dominate winter microcosm experiments

381　(March and December, microcosms 1, 3, 4 and 7, Fig. 6). As discussed above, the community

382　dynamics in the field may have prevented the growth of Mamiellophyceae even under favorable

383　conditions in microcosms. Microcosms on pre-bloom communities (September) led to an

384　increased contribution of *Micromonas* under the winter/ autumn incubation conditions (March,

385　December) even though *Micromonas* ASV contributions were low in September natural

386　communities. Although documented temperature preferences of *Micromonas* Mediterranean

387　strains range between 25 and 30°C [48], we observe that *Micromonas* blooms around 14°C in

388　natural communities and that winter/autumn temperatures and light conditions were more

389　favorable to *Micromonas* in microcosms. The differences in temperature preferenda of

390　*Micromonas* between culture strains and natural communities suggest factors other than

391　temperature such as biotic interactions. Strong light especially may be inhibiting the growth of

392　Mamiellophyceae in microcosms since we never observed Mamiellophyceae in June incubation

393　conditions (similar temperature as in September incubation). Biotic interactions may also

394　influence *Micromonas'* ecological niche, such as parasitism and competition.

395　　　　Experiments 1, 4 and 5 were particularly interesting to investigate the temporal patterns

396　of Chlorophyta that occurred in SOLA natural communities (Fig. 6). Mamiellophyceae, which

397　dominated Chlorophyta in natural communities of March 2015, were still detected together with

398 Chlorodendrophyceae under the low temperature incubation (12.2°C) but Chlorodendrophyceae

399 replaced them in the other microcosms of March 2015. In March 2016, a switch between

400 Mamiellophyceae and Chloropicophyceae occurred under low temperature incubations. These

401 results suggest that (i) the succession of Mamiellophyceae to Chlorodendrophyceae in

402 microcosms reflect their succession in the field and (ii) the switch from Mamiellophyceae to

403 Chlorodendrophyceae occurs independently of temperature and light conditions and is mostly

404 influenced by ecological processes such as biotic interactions. Reads assigned to several grazers

405 such as ciliates or parasites such as Syndiniales were found at that time, but unfortunately no

406 ecological relationships are known between Mamiellophyceae and specific heterotrophic

407 protists. Furthermore viruses (which were not followed in this study) may significantly affect

408 microalgal populations and ecological interactions [7, 49].

Conclusion

410 Our combined approach of microbial diversity monitoring at SOLA together with microcosms

411 simulating seasonal conditions of light and temperature unveiled several aspects of the

412 regulation of phytoplankton seasonality by light and temperature: (1) overall a five days

413 incubation was not sufficient to completely reshape the initial microbial communities, (2) the *in*

414 *situ* dynamics of phytoplankton starting communities modulated the impact of applied seasonal

415 conditions in microcosms as seen for Diatoms or Chlorodendrophyceae in bloom or post-bloom

416 conditions. (3) In pre-bloom conditions, phytoplanktonic species were the most sensitive to light

417 and temperature conditions. Diatoms were favored by higher temperature independently of

418 light, while Mamiellophyceae increased under lower temperatures and lower light intensities

419 (December and March). Altogether, our results suggest that light and temperature seasonal

420 conditions play an importantrole in regulating phytoplankton in pre-bloom conditions and biotic

421 interactions may be preponderant in bloom and post-bloom conditions.

422

REFERENCES

1. Giesbrecht W. Systematik und Faunistik der pelagischen Copepoden des Golfes von Neapel und der angrenzenden Meeres-abschnitte. 1892. R. Friedlander & Sohn, Berlin,.

2. Marino D, Modigh M. An Annotated Check-List of Planktonic Diatoms from the Gulf of Naples. *Mar Ecol* 1981; **2**: 317–333.

3. Péragallo H, Péragallo H, Péragallo M. Diatomées marines de France et des districts maritimes voisins,. 1897. M. J. Tempère, Grez-sur-Loing,.

4. Travers A, Travers M. Les Silicoflagellés du Golfe de Marseille. *Mar Biol* 1968; **1**: 285–288.

5. Daday EJ. Systematische Übersicht der Dinoflagellaten des Golfs von Naples. *Terménez Füzetek* 1888; **11**: 98–109.

6. Throndsen J, Zingone A. Micromonads of the Mediterranean Sea. *G Bot Ital* 1994; **128**: 1031–1044.

7. Zingone A, Sarno D, Forlani G. Seasonal dynamics in the abundance of *Micromonas pusilla* (Prasinophyceae) and its viruses in the Gulf of Naples (Mediterranean Sea). *J Plankton Res* 1999; **21**: 2143–2159.

8. Gomez F, Gorsky G. Annual microplankton cycles in Villefranche Bay, Ligurian Sea, NW Mediterranean. *J Plankton Res* 2003; **25**: 323–339.

9. Lambert S, Tragin M, Lozano JC, Ghiglione JF, Vaulot D, Bouget FY, et al. Rhythmicity of coastal marine picoeukaryotes, bacteria and archaea despite irregular environmental perturbations. *ISME J* 2019; **13**: 388–401.

10. Piredda R, Tomasino MP, D'Erchia AM, Manzari C, Pesole G, Montresor M, et al. Diversity and temporal patterns of planktonic protist assemblages at a Mediterranean Long Term Ecological Research site. *FEMS Microbiol Ecol* 2017; **93**: fiw200.

11. Tragin M, Vaulot D. Green microalgae in marine coastal waters: The Ocean Sampling Day (OSD) dataset. *Sci Rep* 2018; **8**: 14020.

12. Cadier M, Gorgues T, Sourisseau M, Edwards CA, Aumont O, Marié L, et al. Assessing spatial and temporal variability of phytoplankton communities' composition in the Iroise Sea ecosystem (Brittany, France): A 3D modeling approach. Part 1: Biophysical control over plankton functional types succession and distribution. *J Mar Syst* 2017; **165**: 47–68.

13. Thyssen M, Grégori GJ, Grisoni JM, Pedrotti ML, Mousseau L, Artigas LF, et al. Onset of the spring bloom in the northwestern Mediterranean Sea: Influence of environmental pulse events on the in situ hourly-scale dynamics of the phytoplankton community structure. *Front Microbiol* 2014; **5**: 387.

14. Chambouvet A, Morin P, Marie D, Guillou L. Control of Toxic Marine Dinoflagellate Blooms by Serial Parasitic Killers. *Science (80-)* 2008; **322**: 1254–1257.

15. Conan P, Testor P, Estournel C, D'Ortenzio F, Durrieu de Madron X. Observing Winter Mixing and Spring Bloom in the Mediterranean. *Eos (Washington DC)* 2018; **99**.

16. Calvo-Díaz A, Ďaz-Pérez L, Suárez LÁ, Morán XAG, Teira E, Marañón E. Decrease in the autotrophic-to-heterotrophic biomass ratio of picoplankton in oligotrophic marine waters due to bottle enclosure. *Appl Environ Microbiol* 2011; **77**: 5739–5746.

17. Tortell P, DiTullio G, Sigman D, Morel F. CO2 effects on taxonomic composition and nutrient utilization in an Equatorial Pacific phytoplankton assemblage. *Mar Ecol Prog Ser* 2002; **236**: 37–43.

18. Kling JD, Lee MD, Fu F, Phan MD, Wang X, Qu P, et al. Transient exposure to novel high temperatures reshapes coastal phytoplankton communities. *ISME J* 2020; **14**: 413–424.

19. Nielsen LT, Jakobsen HH, Hansen PJ. High resilience of two coastal plankton communities to twenty-first century seawater acidification: Evidence from microcosm studies. *Mar Biol Res* 2010; **6**: 542–555.

20. Hugoni M, Taib N, Debroas D, Domaizon I, Dufournel IJ, Bronner G, et al. Structure of the rare archaeal biosphere and seasonal dynamics of active ecotypes in surface coastal waters. *Proc Natl Acad Sci U S A* 2013; **110**: 6004–6009.

21. Stoeck T, Bass D, Nebel M, Christen R, Jones MDM, Breinner H-W, et al. Multiple marker parallel tag environmental DNA sequencing reveals a highly complex eukaryotic community in marine anoxic water. *Mol Ecol* 2010; **19**: 21–31.

22. Callahan BJ, McMurdie PJ, Rosen MJ, Han AW, Johnson AJA, Holmes SP. DADA2: High-resolution sample inference from Illumina amplicon data. *Nat Methods* 2016; **13**: 581–583.

23. Schloss PD, Westcott SL, Ryabin T, Hall JR, Hartmann M, Hollister EB, et al. Introducing mothur: open-source, platform-independent, community-supported software for describing and comparing microbial communities. *Appl Environ Microbiol* 2009; **75**: 7537–41.

24. Guillou L, Bachar D, Audic S, Bass D, Berney C, Bittner L, et al. The Protist Ribosomal Reference database (PR2): A catalog of unicellular eukaryote Small Sub-Unit rRNA sequences with curated taxonomy. *Nucleic Acids Res* 2013; **41**: 597–604.

25. Tragin M, Lopes dos Santos A, Christen R, Vaulot D, Massana R. Diversity and ecology of green microalgae in marine systems: an overview based on 18S rRNA gene sequences. *Perspect Phycol* 2016; **3**: 141–154.

26. Edvardsen B, Egge ES, Vaulot D. Diversity and distribution of haptophytes revealed by environmental

493   sequencing and metabarcoding – a review. *Perspect Phycol* 2016; **3**: 77–91.

494 27. Mordret S, Piredda R, Vaulot D, Montresor M, Kooistra WHCF, Sarno D. dinoref : A curated dinoflagellate

495   (Dinophyceae) reference database for the 18S rRNA gene. *Mol Ecol Resour* 2018; **18**: 974–987.

496 28. Simpson EH. Measurement of diversity. *Nature* 1949; **163**: 688–688.

497 29. Clarke KR. Non‐parametric multivariate analyses of changes in community structure. *Aust J Ecol* 1993; **18**:

498   117–143.

499 30. Pereira O, Hochart C, Boeuf D, Auguet JC, Debroas D, Galand PE. Seasonality of archaeal proteorhodopsin

500   and associated Marine Group IIb ecotypes (Ca. Poseidoniales) in the North Western Mediterranean Sea.

501   *ISME J* 2020.

502 31. Massana R, del Campo J, Sieracki ME, Audic S, Logares R. Exploring the uncultured microeukaryote

503   majority in the oceans: reevaluation of ribogroups within stramenopiles. *ISME J* 2014; **8**: 854–66.

504 32. Guillou L, Viprey M, Chambouvet A, Welsh RM, Kirkham AR, Massana R, et al. Widespread occurrence

505   and genetic diversity of marine parasitoids belonging to Syndiniales (Alveolata). *Environ Microbiol* 2008;

506   **10**: 3349–3365.

507 33. Peterfi LS, Manton I. Observations with the electron microscope on Asteromonas gracilis Artari emend. (

508   Stephanoptera gracilis (Artari) wisl.), with some comparative observations on Dunaliella Sp. *Br Phycol Bull*

509   1968; **3**: 423–440.

510 34. Gómez F. A quantitative review of the lifestyle, habitat and trophic diversity of dinoflagellates

511   (Dinoflagellata, Alveolata). *Syst Biodivers* 2012; **10**: 267–275.

512 35. Zhu F, Massana R, Not F, Marie D, Vaulot D, Ishizaka J, et al. Mapping of picoeucaryotes in marine

513   ecosystems with quantitative PCR of the 18S rRNA gene. *FEMS Microbiol Ecol* 2005; **52**: 79–92.

514 36. Gong W, Marchetti A. Estimation of 18S gene copy number in marine eukaryotic plankton using a next-

515   generation sequencing approach. *Front Mar Sci* 2019; **6**.

516 37. Massana R, Gobet A, Audic S, Bass D, Bittner L, Boutte C, et al. Marine protist diversity in European

517   coastal waters and sediments as revealed by high-throughput sequencing. *Environ Microbiol* 2015; **17**:

518   4035–4049.

519 38. Malviya S, Scalco E, Audic S, Vincent F, Veluchamy A, Poulain J, et al. Insights into global diatom

520   distribution and diversity in the world's ocean. *Proc Natl Acad Sci U S A* 2016; **113**: E1516-25.

521 39. Gómez F, Gorsky G. Annual microplankton cycles in Villefranche Bay, Ligurian Sea, NW Mediterranean. *J*

522   *Plankton Res* 2003; **25**: 323–339.

523 40. Vaulot D, Eikrem W, Viprey M, Moreau H. The diversity of small eukaryotic phytoplankton (≤3 μm) in

524   marine ecosystems. *FEMS Microbiol Rev* 2008; **32**: 795–820.

525 41. Zingone A, D'Alelio D, Mazzocchi MG, Montresor M, Sarno D, Balestra C, et al. Time series and beyond:

526   Multifaceted plankton research at a marine Mediterranean LTER site. *Nat Conserv* 2019; **34**: 273–310.

527 42. Leblanc K, Quéguiner B, Diaz F, Cornet V, Michel-Rodriguez M, Durrieu De Madron X, et al.

528   Nanoplanktonic diatoms are globally overlooked but play a role in spring blooms and carbon export. *Nat*

529   *Commun* 2018; **9**.

530 43. del Campo J, Not F, Forn I, Sieracki ME, Massana R. Taming the smallest predators of the oceans. 2013.

531 44. Gieskes WWC, Kraay GW, Baars MA. Current 14C methods for measuring primary production: Gross

532   underestimates in oceanic waters. *Netherlands J Sea Res* . 1979. Elsevier. , **13**: 58–78

533 45. Not F, Latasa M, Marie D, Cariou T, Vaulot D, Simon N. A single species, *Micromonas pusilla*

534   (Prasinophyceae), dominates the eukaryotic picoplankton in the Western English Channel. *Appl Environ*

535   *Microbiol* 2004; **70**: 4064–72.

536 46. Schiller J. Vorläufige Ergebnisse der Phytoplanktonuntersuehungen auf den Fahrten S. M.S. 'Najade' in der

537   Adria. II. Flagellaten und Chlorophyceen. *Sitzungsberichte der Akad der Wissenschaften Wien, Math Klasse*

538   1913; **122**: 621–63.

539 47. Throndsen J, Zingone A. *Tetraselmis wettsteinii* (Schiller) throndsen comb. nov. and its occurrence in golfo

540   di napoli. *G Bot Ital* 1988; **122**: 227–235.

541 48. Demory D, Baudoux AC, Monier A, Simon N, Six C, Ge P, et al. Picoeukaryotes of the Micromonas genus:

542   sentinels of a warming ocean. *ISME J* 2019; **13**: 132–146.

543 49. Fuhrman JA. Marine viruses and their biogeochemical and ecological effects. *Nature* . 1999. , **399**: 541–548

544

545 **Figure Legends**

546 **Fig. 1**: Description of the microcosm experimental procedure. Sea water was sampled 3 to 4

547 times a year in 2015 and 2016 at SOLA SOMLIT station off Banyuls-sur-mer (France). The 7

548 seawater samples were incubated in artificial conditions mimicking average seasons. Each

549 experiment was re-named by a code combining the sampling date (1 to 7) and the incubation

550 conditions code. Incubation codes were 0 to 5: 0 was SOLA control sample, 1 to 4 refers to

551 incubation conditions (spring – green - 1, summer – yellow - 2, autumn – red - 3 and winter –

552 blue - 4) and 5 refers to SOLA next control sample (4 to 10 days after initial sampling).

553 **Fig. 2:** Treemaps representing the distribution of V4 region of the 18S rRNA gene

554 metabarcodes in supergroups and major divisions of marine protists. Bold legends refer to

555 lineages hosting photosynthetic protists. A- Global taxonomic diversity in the 56 microcosm

556 samples, B- Global taxonomic diversity in 140 SOLA times series samples.

557 **Fig. 3:** Number of ASV per microcosm samples versus the Simpson diversity index. Only

558 ASVs represented by more than 10 reads and sample with more than 4000 sequenced reads

559 were taken into account. Each dot and label correspond to a microcosm experiment number.

560 Colors represent the month when the sea water was sampled and the dot shape represent either

561 the nutriment conditions (incubation with Nitrate and Phosphate enrichment) or the natural

562 samples from environmental time series (bold labels). Labels refer to the sampling-incubation

563 condition codes as defined in Fig. 1 and Supplementary Table 1.

564 **Fig. 4:** Non-parametric Multi-Dimensional Scaling (NMDS) representing microcosm

565 experiment and natural samples protist communities. The NMDS calculation was based on a

566 Bray-Curtis distance matrix and resulted in an acceptable stress value (0.2039). Only ASVs

567 represented by more than 10 reads and sample with more than 4000 sequenced reads were taken

568 into account. No environmental parameters are plotted on the NMDS graphic since none had a

569   P-value (100 permutations) lower than 0.05. Labels refers to the sampling-incubation condition

570   codes as defined in Fig. 1 and Supplementary Fig.1 and the dot shape represents either the

571   nutriment conditions (incubation with Nitrate and Phosphate enrichment) or the natural samples

572   from environmental time series (bold labels). A- Colors represents the month when the sea

573   water was sampled. B- Colors represent the incubation conditions (artificial month: temperature

574   and daylight length mimicking seasons).

575   **Fig. 5:** Barplot representing the percentage of reads assigned to each eukaryotic taxonomic

576   supergroup in microcosm incubated without Nitrate and Phosphate enrichment and natural

577   samples. Sequences assigned to Metazoans were deleted from the dataset. Colors in the barplot

578   refer to supergroups, colors in the legend correspond to the month, when the initial sea water

579   was sample and letters (in grey) to the incubation conditions (i.e. artificial month): March (M),

580   June (J), September (S) and December (D). A- Natural and incubated samples from March 2015

581   and 2016. B- Natural and incubated samples from June 2015 and 2016. C- Natural and

582   incubated samples from December 2015 and 2016. D- Natural and incubated samples from
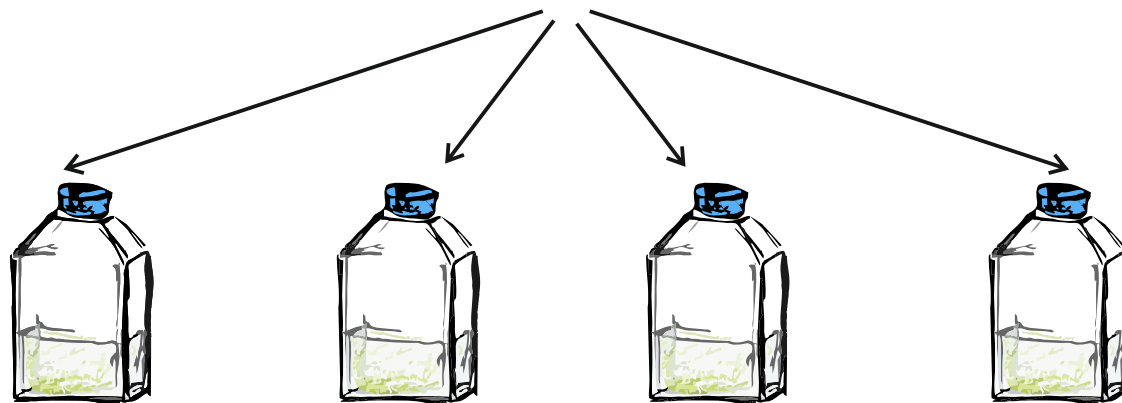
583   September 2016.

584   **Fig. 6:** Chlorophyta classes contribution: A- Relative contribution of Chlorophyta classes (%) in

585   the SOLA environmental high sampling frequency time series. Grey dots and lines point out the

586   sampling date of sea water incubated for microcosm experiments. B- Barplots represent the

587   number of reads per Chlorophyta classes in the 4 microcosm experiments and their associated

588   natural sample. Colors in the barplot refer to Chlorophyta classes, colors in the legend

589   correspond to the month, when the initial sea water was sample and letters (in grey) to the

590   incubation conditions (i.e. artificial month): March (M), June (J), September (S) and December

591   (D).

2015 **2016**

Winter	Spring	Summer	Autumn	Winter	Spring	Summer	Autumn

Samples code 1 2 3 4 5 6 7
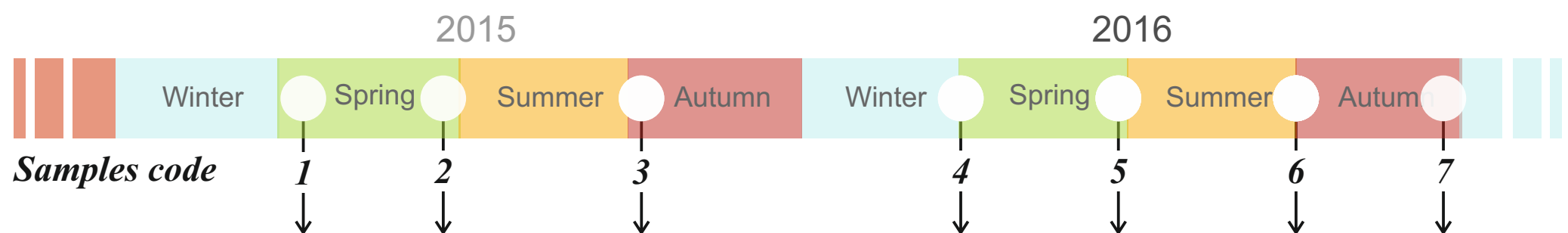
7 Natural seawater samples (Banyuls Bay)
400 ml (x3), pre-filtration on 3 μm

Nomenclature:

- **10** sampled March 30. 2015, no incubation, SOLA control.

- **11** sampled March 30. 2015 and incubated in March artificial conditions.

- **12** sampled March 30. 2015 and incubated in June artificial conditions.

- **15** sampled March 30. 2015, no incubation, « final » SOLA control sample.

5 days incubation

Incubation code	*1*	*2*	*3*	*4*
Artificial season	March	June	September	December
Temperature (°C)	12.2	18.8	20.7	14.4
Day length (h)	11.95	14.75	12.08	9.13
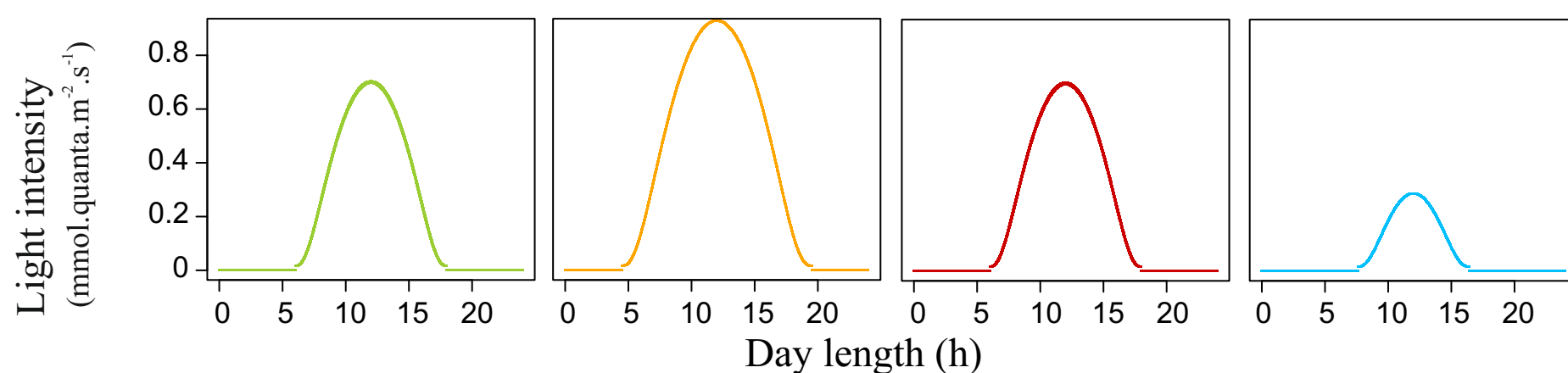
Filtration, extraction, PCR and sequencing

- **0.22 μm** sterivex

- **V4** region of the **18S rRNA gene** (Piredda *et al.* 2017):
  Forward [5'-CCAGCASCYGCGGTAATTCC]
  Reverse [5'-ACTTTCGTTCTTGATYRATGA]

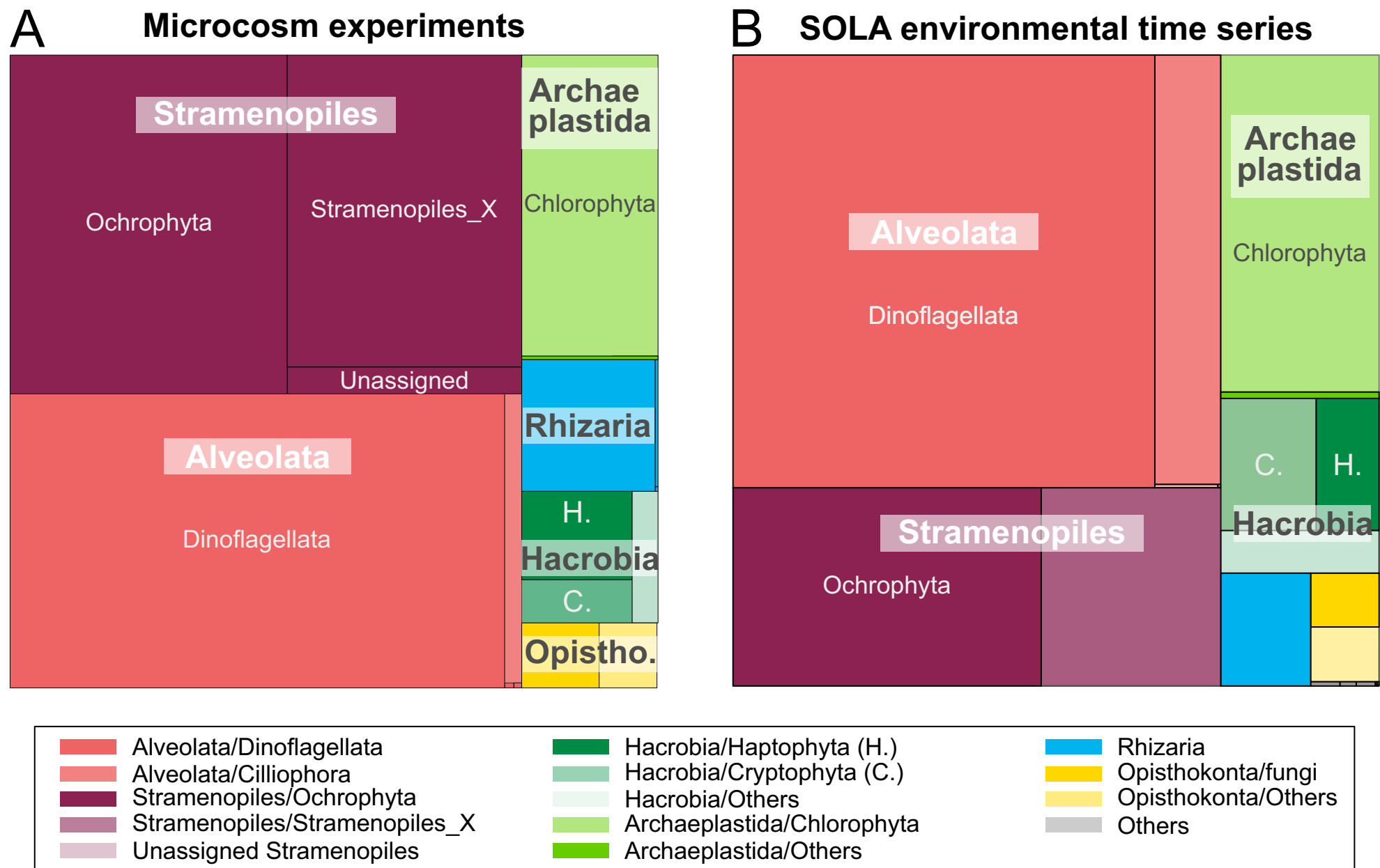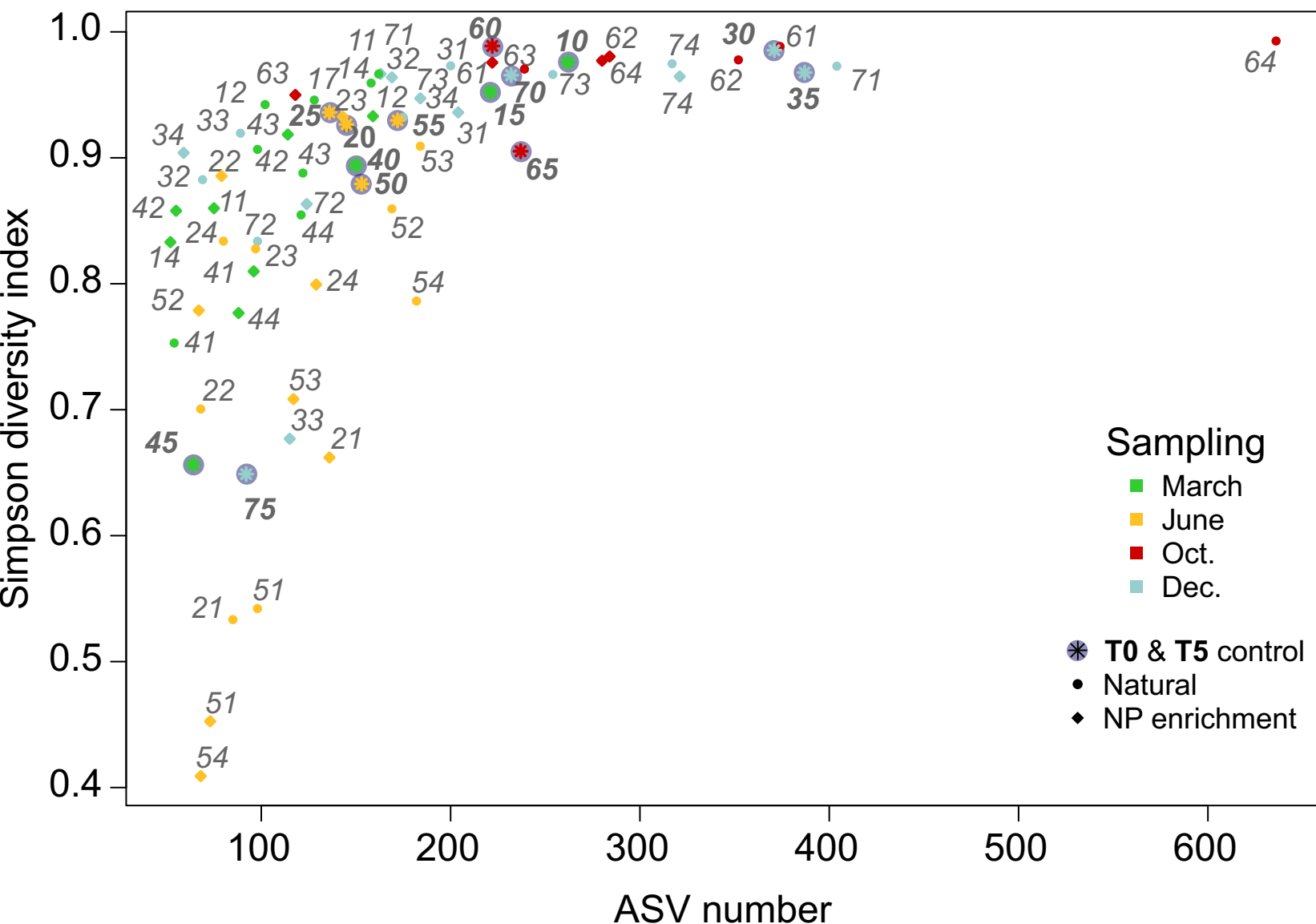- **Illumina** Miseq (250 base pairs x2)

Figure 1

A **Microcosm experiments**
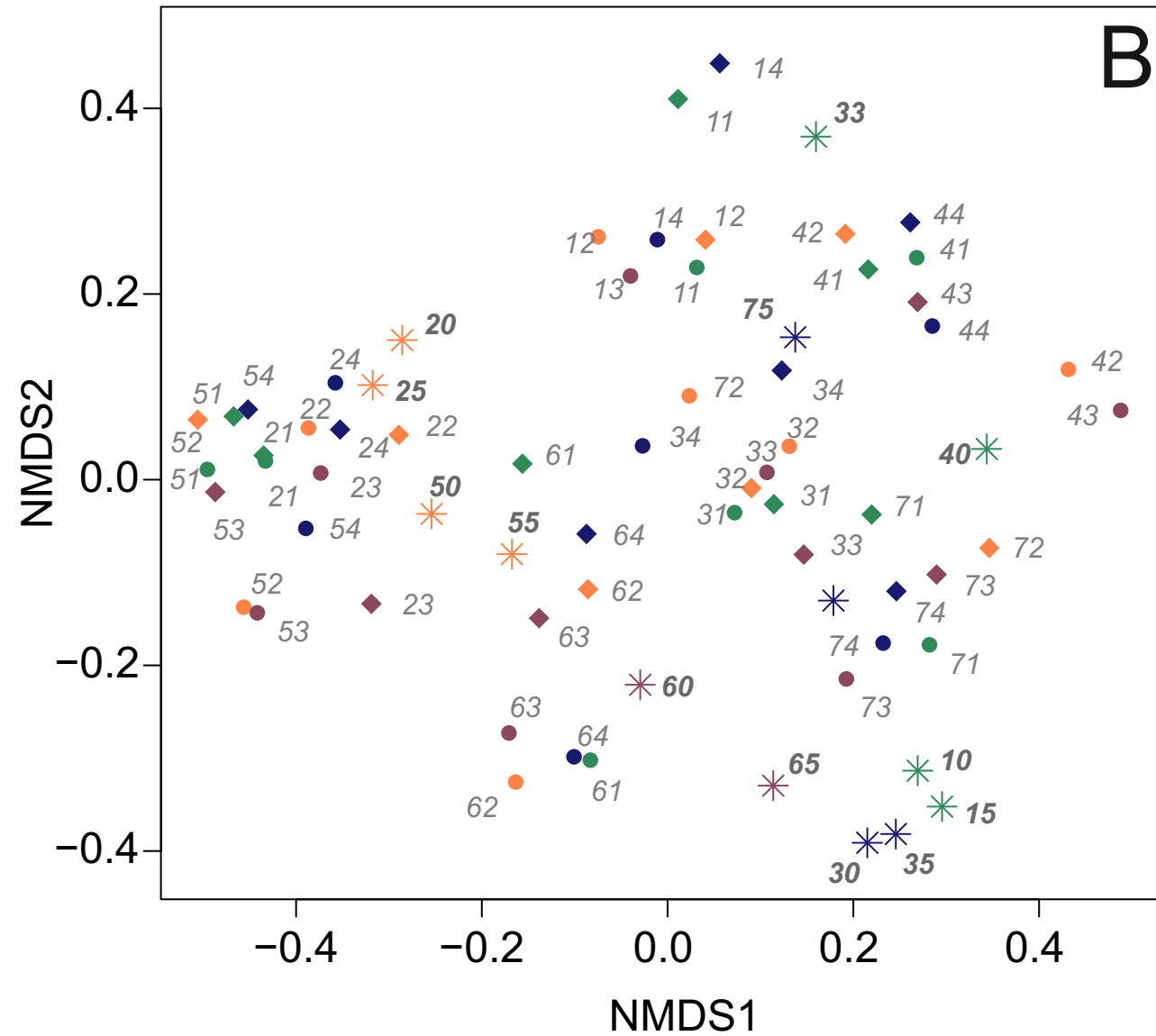
Stramenopiles
Ochrophyta
Stramenopiles_X
Unassigned
Archae plastida
Chlorophyta
Rhizaria
H.
Hacrobia
C.
Alveolata
Dinoflagellata
Opistho.

B **SOLA environmental time series**

Alveolata
Dinoflagellata
Archae plastida
Chlorophyta
C.
H.
Hacrobia
Stramenopiles
Ochrophyta

Legend:
- Alveolata/Dinoflagellata
- Alveolata/Cilliophora
- Stramenopiles/Ochrophyta
- Stramenopiles/Stramenopiles_X
- Unassigned Stramenopiles
- Hacrobia/Haptophyta (H.)
- Hacrobia/Cryptophyta (C.)
- Hacrobia/Others
- Archaeplastida/Chlorophyta
- Archaeplastida/Others
- Rhizaria
- Opisthokonta/fungi
- Opisthokonta/Others
- Others

Figure 2

Figure 3

Figure 4
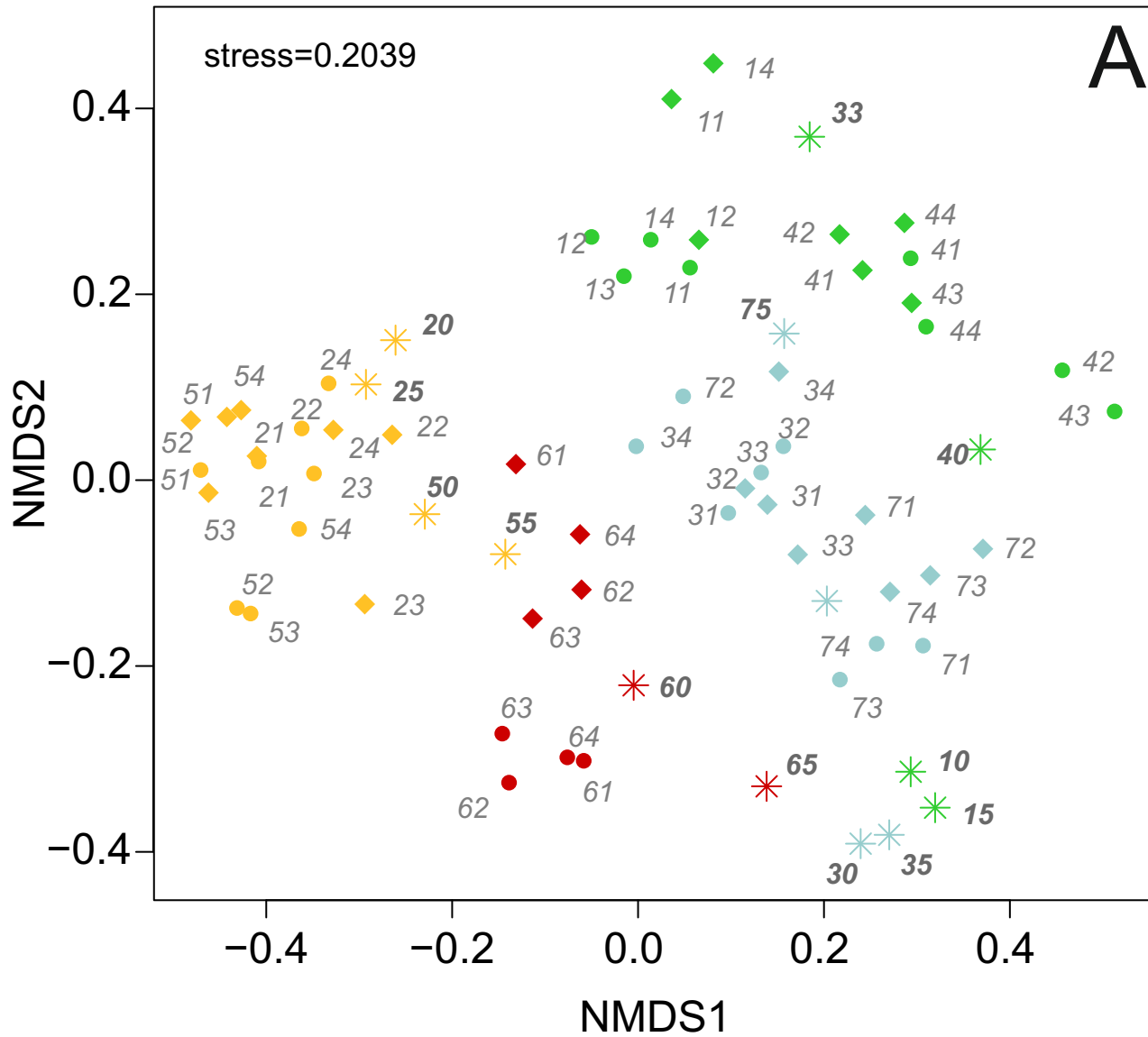
Figure 5

Supergroup of eukaryotes
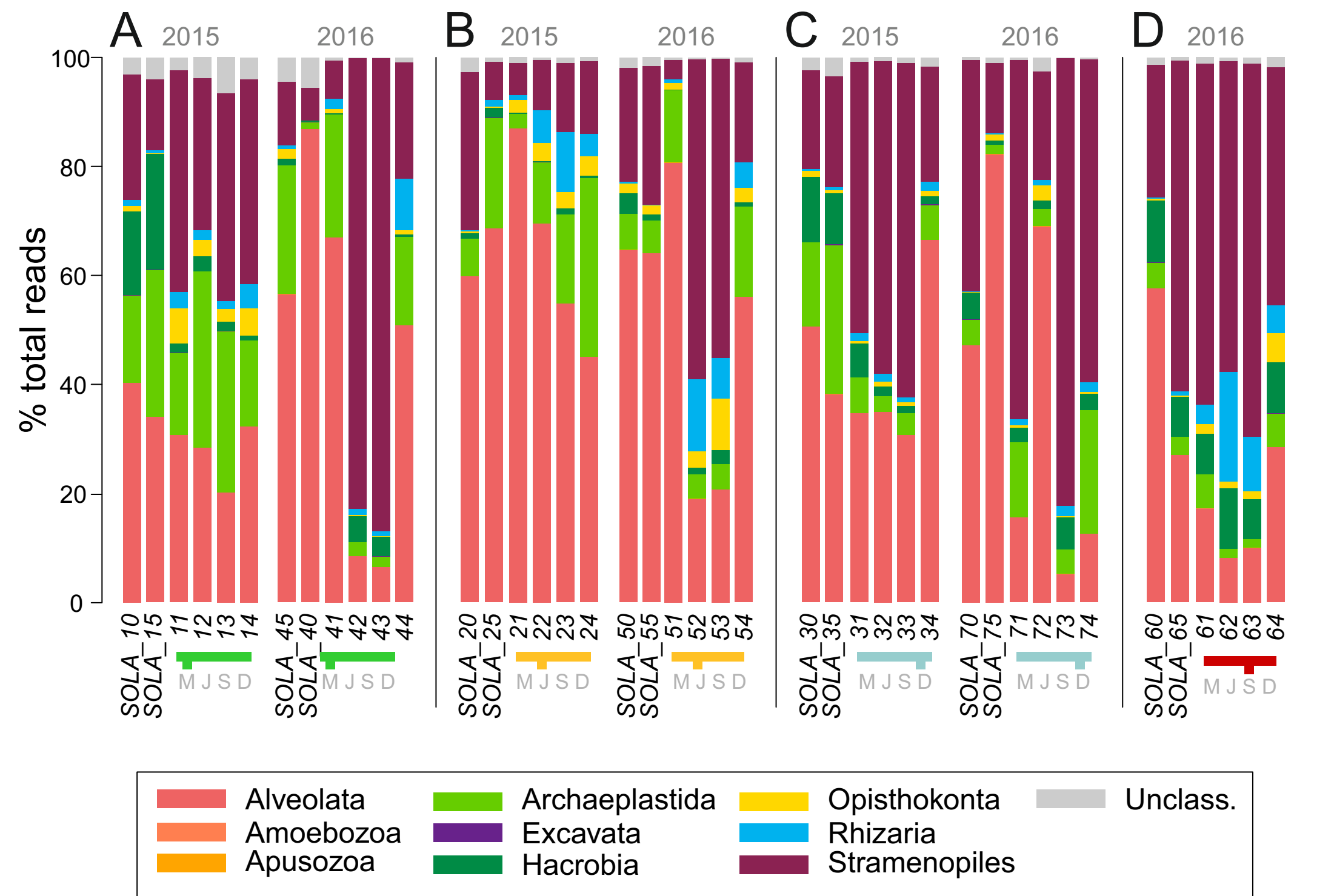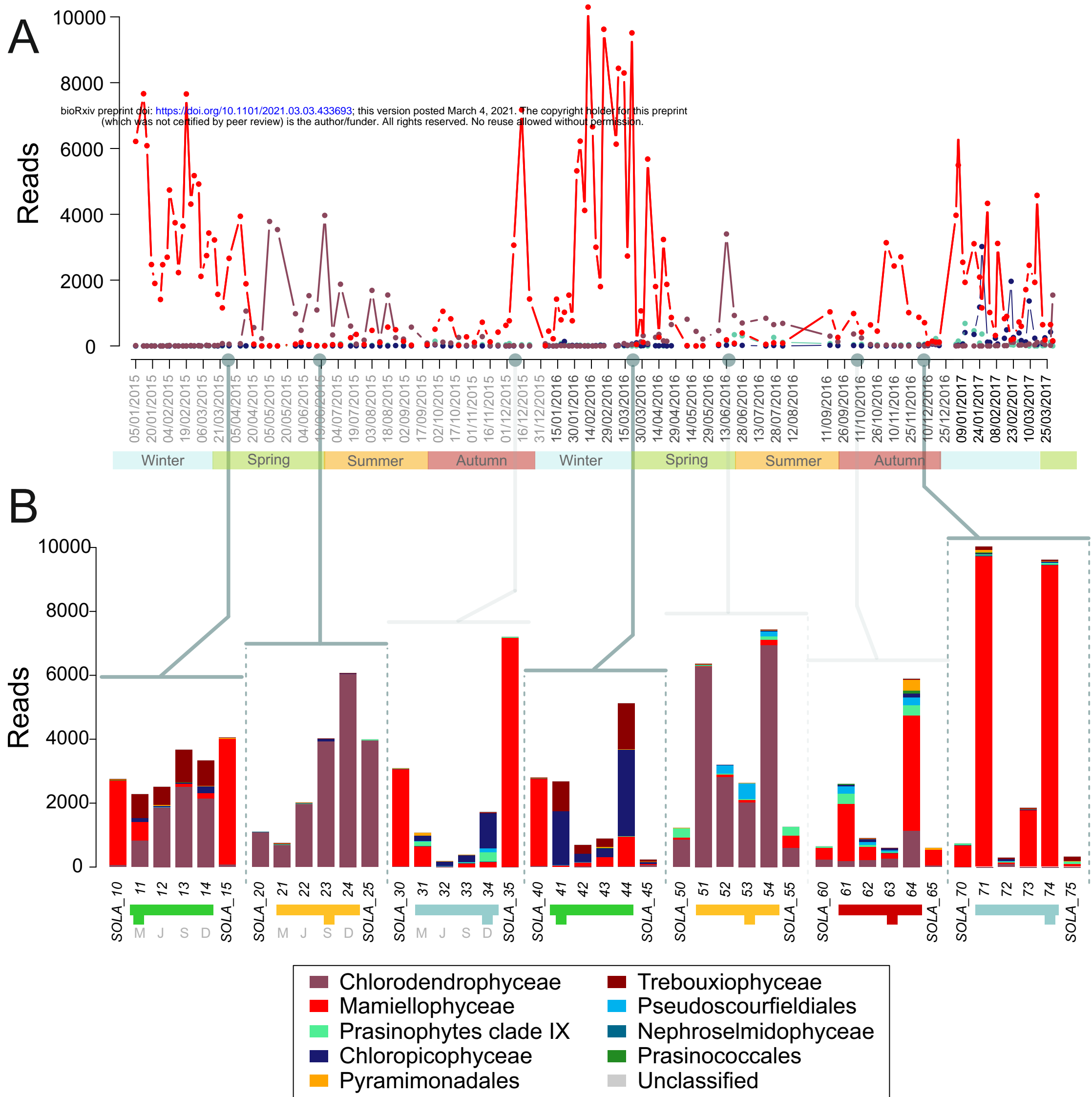
Figure 6

1 **Supplementary Information**

2 **Supplementary Table 1:** Microcosms experimental conditions. 'Sample' was the original

3 sample names, that were translated into a two digit code 'Code'. Sample names starting by

4 'SOLA_' are natural control samples extracted from the environmental time series. 'Sequencing

5 Date' refers to the date of sea water filtration after 5 days incubations to prepare DNA

6 extraction. 'Artificial month' refers to the light and temperatures incubation conditions:

7 Daylight duration ranged from 9.13 hours in December to 14.75 hours in June, with maximum

8 light intensity between 0.3 and 0.9 mmol.quanta.m^{-2}.s^{-1} corresponding to the 3 meter depth of

9 sampling at SOLA. Applied temperature corresponded to the average temperature of the sea at

10 SOLA recorded between 2007 and 2014: in March (12.2 °C), June (18.8 °C), September (20.7

11 °C) and December (14.4 °C). The nutrients enrichment are coded as a Boolean variable, T- 5

12 µM of NaNO$_3$ and 0.2 µM of Na$_2$HPO$_4$ (SIGMA Aldrich) were added to microcosms (NP

13 microcosms) versus F- no nutriments supplementation. All microcosms were sampled at the

14 surface.

15 **Supplementary Table 2**: ASVs table of microcosm experiments and control natural samples:

16 PR² taxonomy and number of reads per samples.

17 **Supplementary Table 3:** Set of eight tables summarizing pairwise simper statistical test: the

18 composition of each of the 6 samples belonging to the same microcosm experiment

19 (microcosms 1 to 7) was compared as well as the March natural samples (1-0, 1-5, 4-0, 4-5).

20 The taxonomical assignation of the ASVs, which influenced the most the dissimilarities

21 between microcosms, are listed next to each table and cumulative dissimilarity % value

22 represented by the 4 top ASVs is mentioned inside the tables.

23 **Supplementary Figure 1:** Evolution of eukaryotic photosynthetic cell numbers (pico- and

24 nano-phytoplankton communities) during microcosm experiments incubation followed by flow

25 cytometry measurements. The colors of the dots refers to incubation condition and the label

26 corresponds to sampling-incubation condition codes as defined in Fig. 1 and Supplementary

27 Table 1**Supplementary Information**

28 **Supplementary Table 1**. **A-** Microcosms incubated without nutrients supplementation. **B-**

29 Microcosms experiments enriched with nitrate and phosphate.

30 **Supplementary Figure 2:** Seasonal patterns of reads assigned to protists taxonomic groups in

31 SOLA environmental high-frequency time series. Grey dots correspond to the sampling dates of

32 sea water for microcosms experiments. **A-** Pattern of abundance of the V4 metabarcodes

33 assigned to the nine eukaryotic supergroups. Metabarcodes assigned to Metazoan were not

34 deleted from the Opisthokonta. Photosynthetic supergroups are in bold in the legend. **B-** Pattern

35 of abundance of the numbers of the V4 metabarcodes assigned to the four major photosynthetic

36 divisions (dinoflagellates excluded).

37 **Supplementary Figure 3:** Seasonal patterns of reads assigned to Ochrophyta microalgae

38 (photosynthetic division of Stramenopiles) in SOLA environmental high-frequency time series.

39 Grey dots correspond to the sampling dates of sea water for microcosms experiments. **A-**

40 Pattern of abundance of the V4 metabarcodes assigned to Ochrophyta classes. **B-** Pattern of

41 abundance of V4 metabarcodes assigned to Bacillariophyta (Ochrophyta) families, **C-** Pattern of

42 abundance of the numbers of the V4 metabarcodes assigned to the Bacillariophyta genera. The

43 most abundant genera are in bold in the legend.

44 **Supplementary Figure 4:** Mamiellophyceae genera contribution in SOLA environmental time

45 series and microcosms. **A-** Seasonal patterns of reads assigned to Mamiellophyceae genera at

46 SOLA. Note that only the two most abundant genera *Micromonas* and *Bathycoccus* can be seen

47   on the graph. Grey dots correspond to the sampling dates of sea water for microcosms

48   experiments. **B-** Barplot representing the number of reads per Mamiellophyceae genera in 4

49   microcosm experiments and their associated natural sample. Colors in the barplot refer to

50   Mamiellophyceae genera, colors in the legend correspond to the month, when the initial sea

51   water was sample and letters (in grey) to the incubation conditions (i.e. artificial month): March

52   (M), June (J), September (S) and December (D).

53

54   **Supplementary Data 1:** Script used to compute and plot ASVs richness versus Simpson's

55   diversity index (Fig. 2) as *Rmarkdown.html* file.

56   **Supplementary Data 2:** Script used to compute and plot (Fig. 3) as *Rmarkdown.html* file.

57   **Supplementary Data 3:** Script used to compute and draw barplots (Fig. 4, Fig. 5B and Fig. S
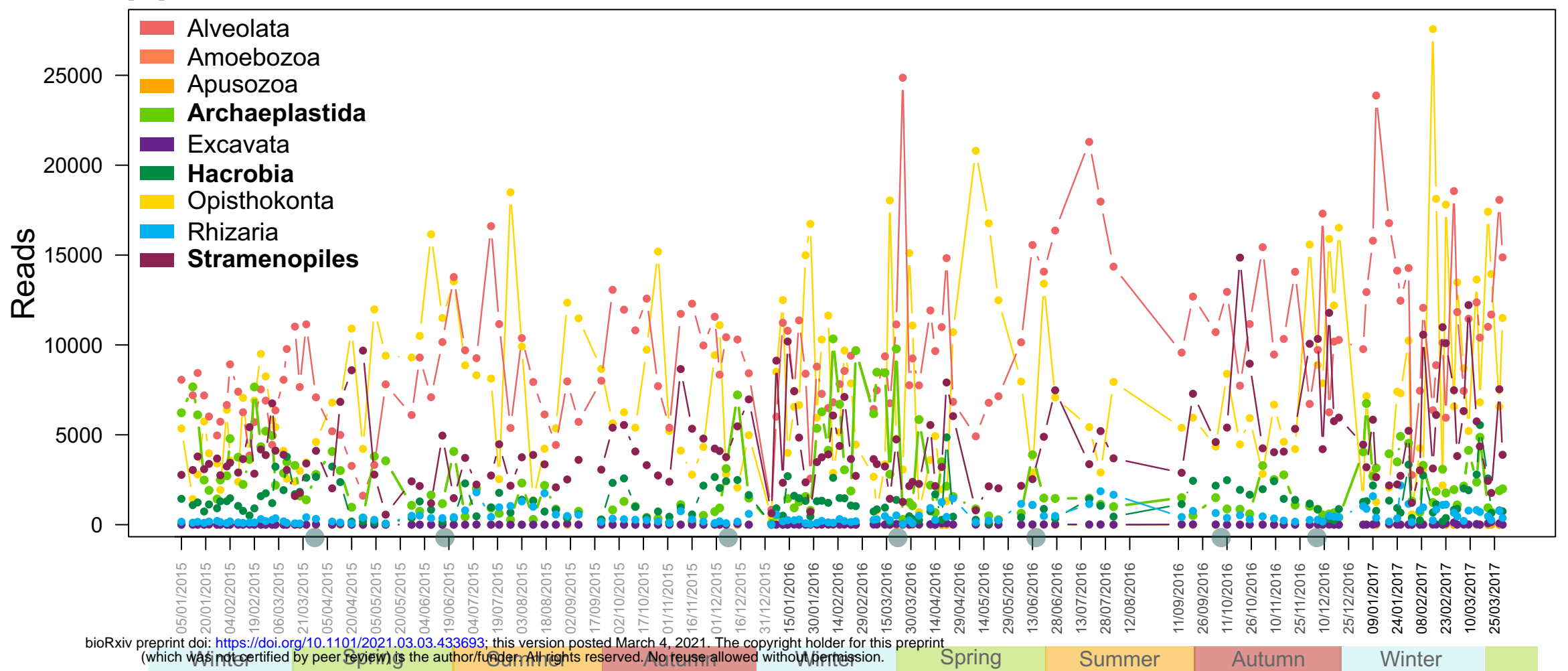
58   5B) as *Rmarkdown.html* file.

59   **Supplementary Data 3:** Script used to compute and plot Treemap (Supplementary figure 2) as

60   *Rmarkdown.html* file.

61   **Supplementary Data 5:** Script used to plot Fig. 5A, Supplementary figures 3 to 6 as
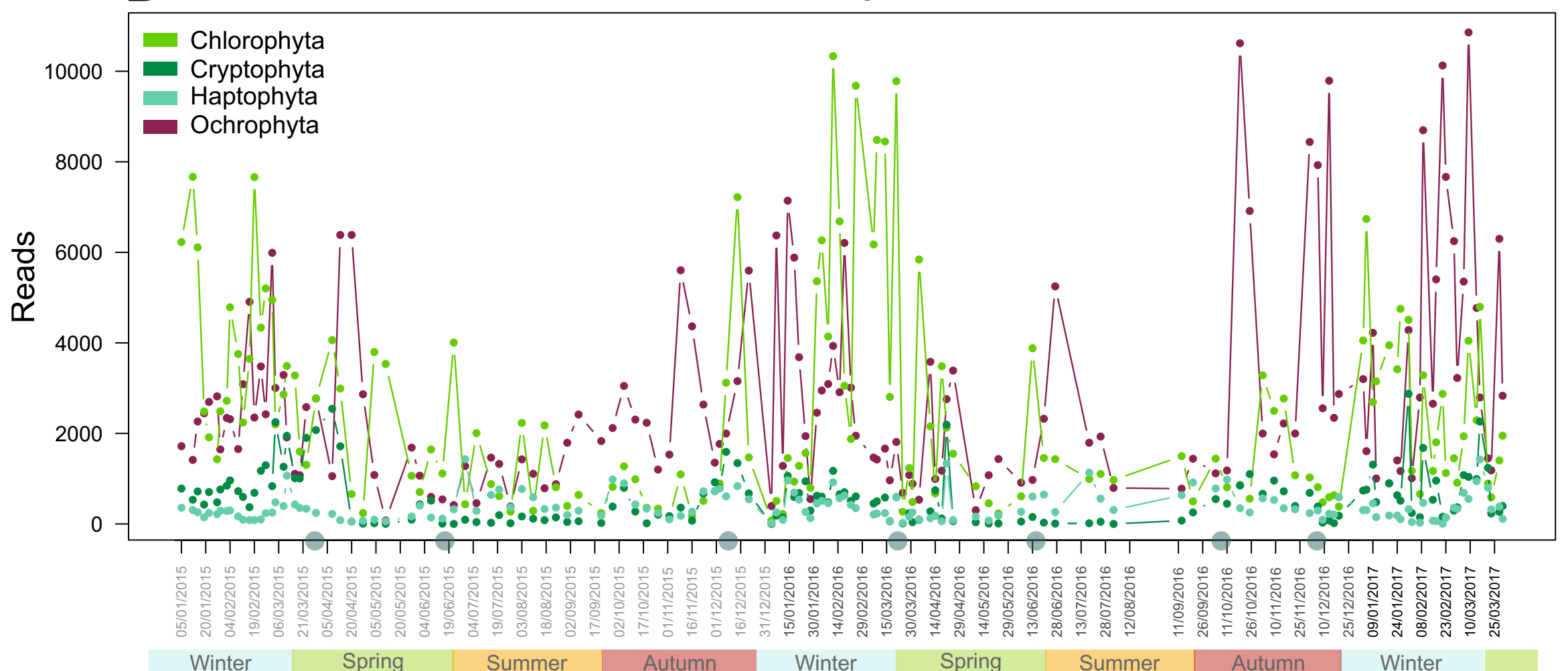
62   *Rmarkdown.html* file.
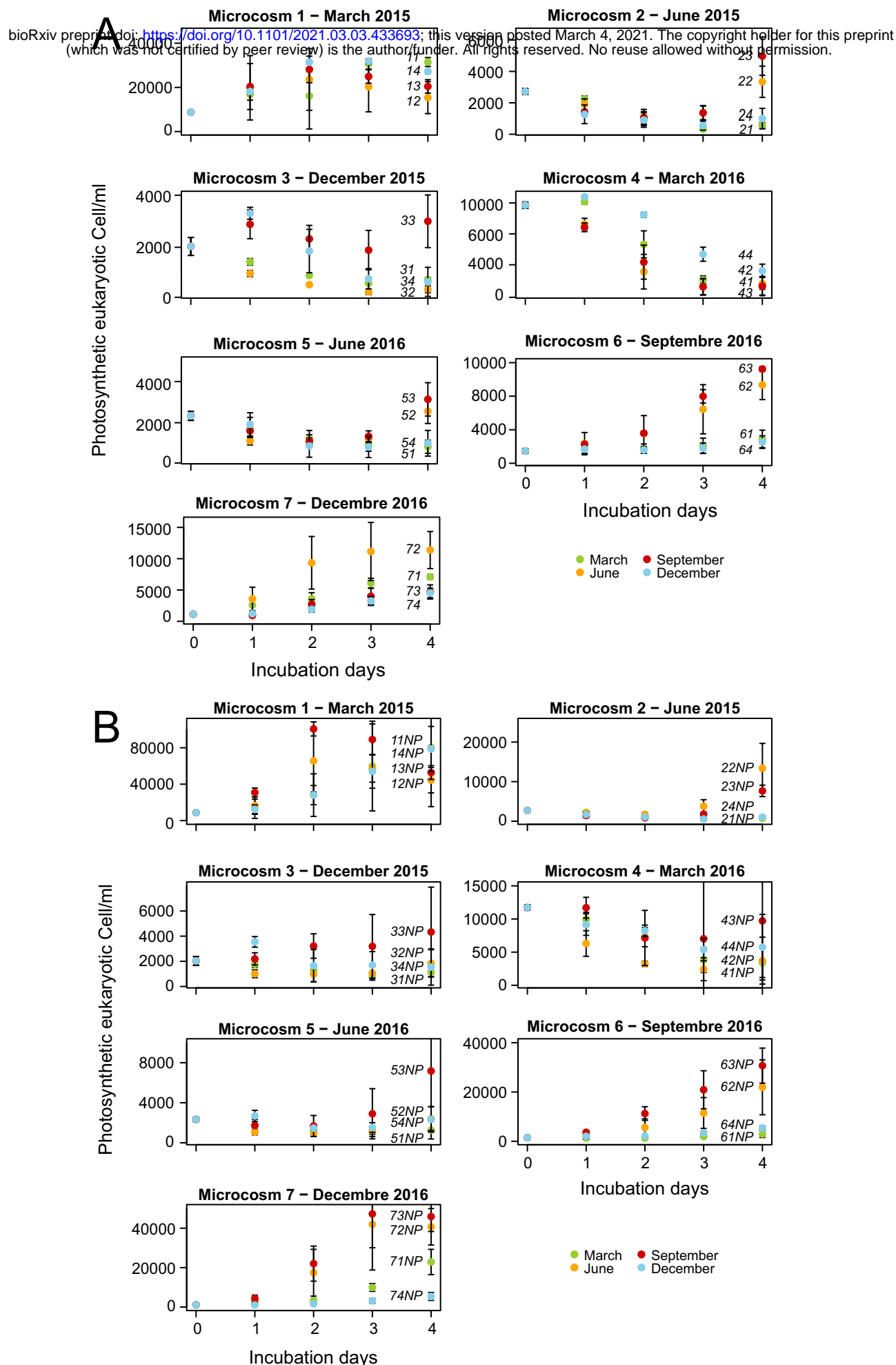
Supplementary Figure 1: Evolution of eukaryotic photosynthetic cell numbers (pico- and nano-phytoplankton communities) during microcosm experiments incubation followed by flow cytometry measurements. The colors of the dots refers to incubation condition and the label corresponds to sampling-incubation condition codes as defined in Fig. 1 and Supplementary Table 1. **A-** Microcosms incubated without nutrients supplementation. **B-** Microcosms experiments enriched with nitrate and phosphate.

A SOLA - Nine eukaryotic Supergroups

Legend:
- Alveolata
- Amoebozoa
- Apusozoa
- **Archaeplastida**
- Excavata
- **Hacrobia**
- Opisthokonta
- Rhizaria
- **Stramenopiles**

B SOLA - Four photosynthetic divisions

Legend:
- Chlorophyta
- Cryptophyta
- Haptophyta
- Ochrophyta

Supplementary Figure 2: Seasonal patterns of reads assigned to protists taxonomic groups in SOLA environmental high-frequency time series. Grey dots correspond to the sampling dates of sea water for microcosms experiments. **A-** Pattern of abundance of the V4 metabarcodes assigned to the nine eukaryotic Supergroups. Metabarcodes assigned to Metazoan were not deleted from the Opisthokonta. Photosynthetic supergroups are in bold in the legend. **B-** Pattern of abundance of the numbers of the V4 metabarcodes assigned to the four major photosynthetic Divisions (dinoflagellates excluded).
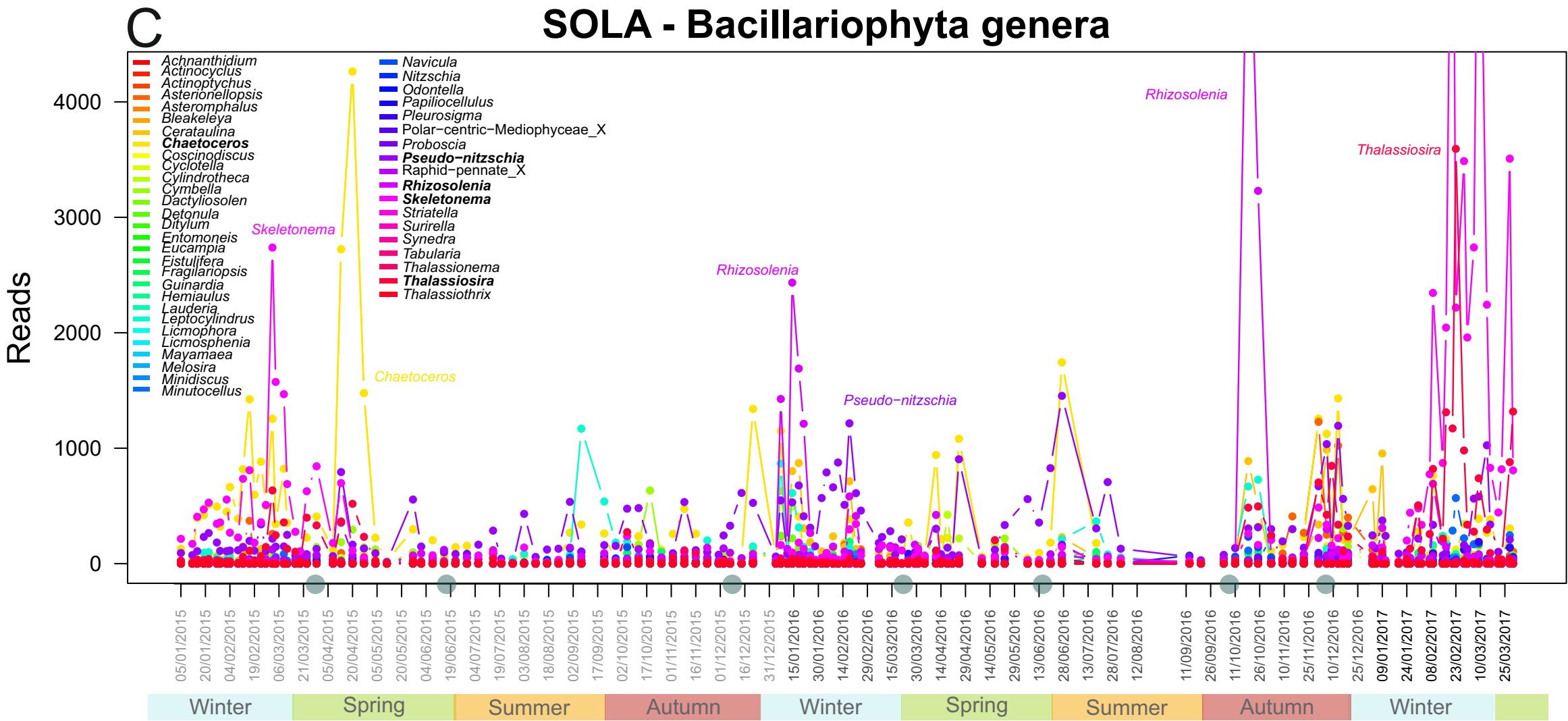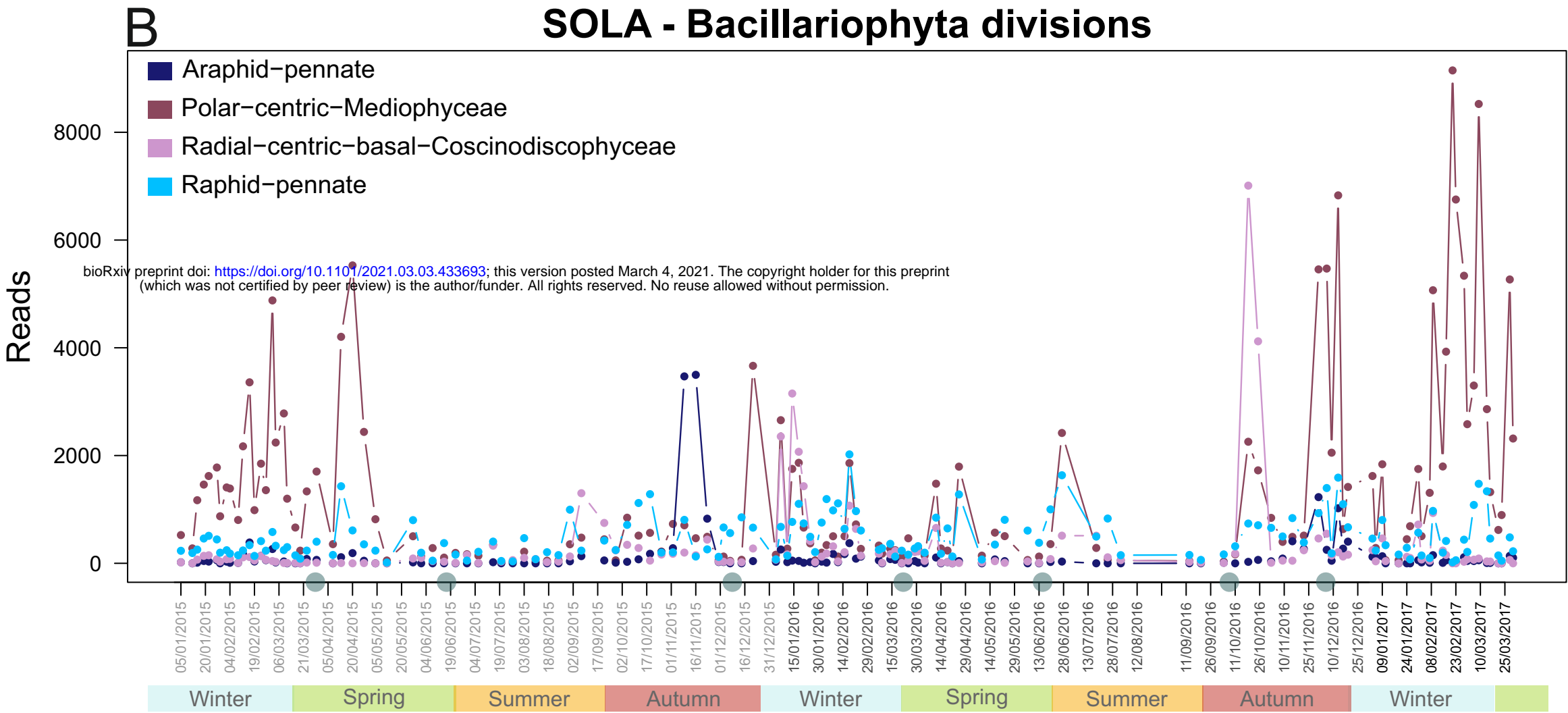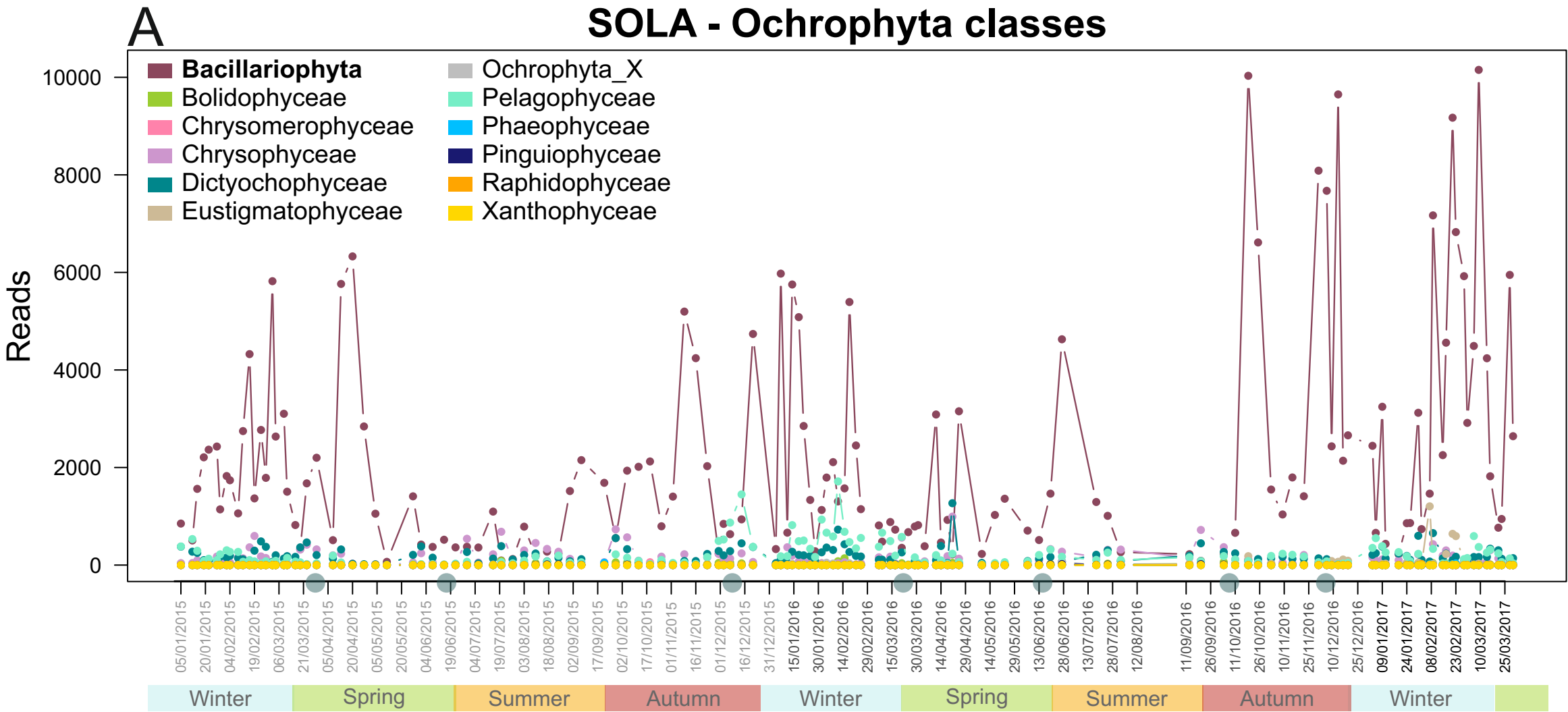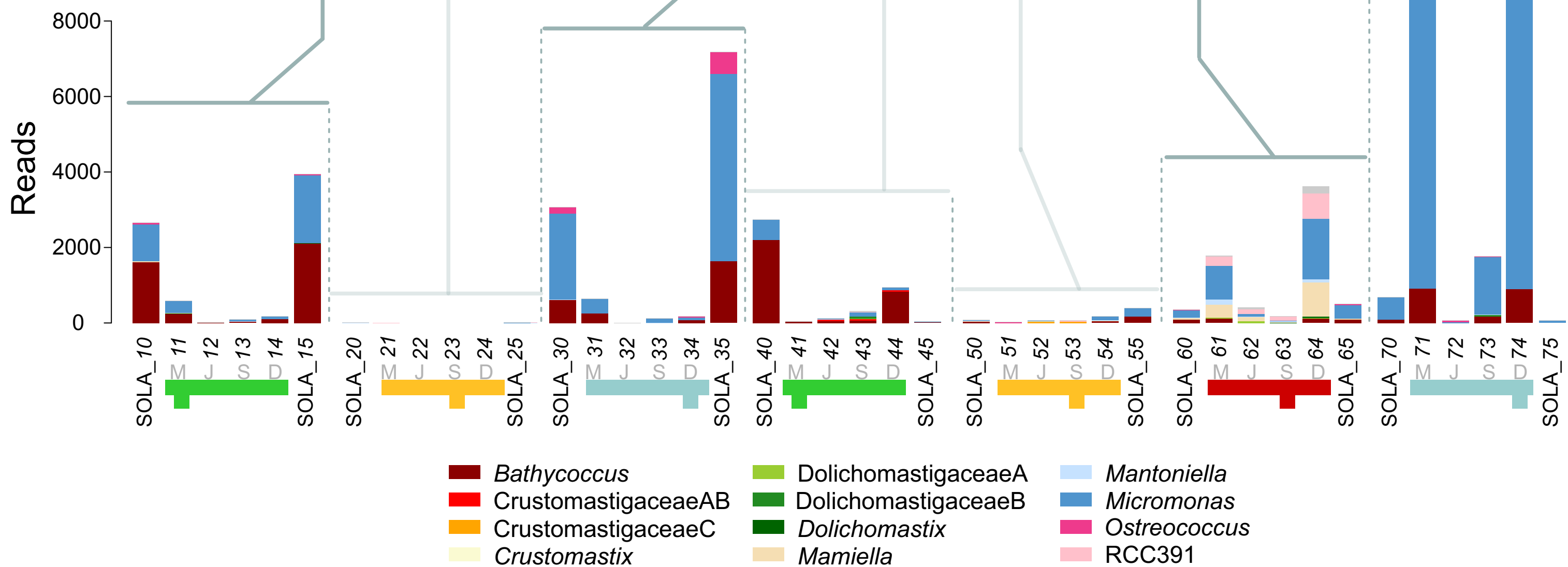
Supplementary Figure 3: Seasonal patterns of reads assigned to Ochrophyta microalgae (photosynthetic division of Stramenopiles) in SOLA environmental high-frequency time series. Grey dots correspond to the sampling dates of sea water for microcosms experiments. **A-** Pattern of abundance of the V4 metabarcodes assigned to Ochrophyta Classes. **B-** Pattern of abundance of V4 metabarcodes assigned to Bacillariophyta (Ochrophyta) families, **C-** Pattern of abundance of the numbers of the V4 metabarcodes assigned to the Bacillariophyta genera. The most abundant genera are in bold in the legend.
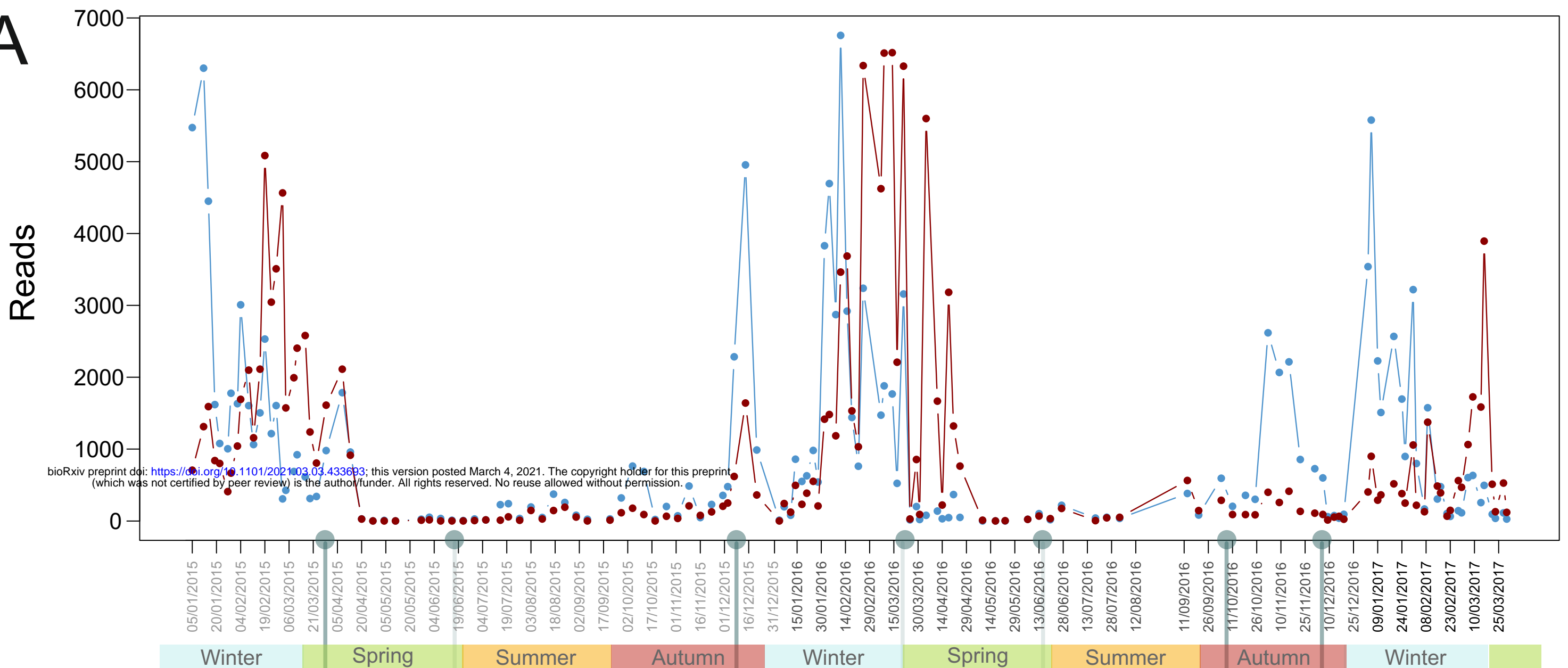
Supplementary Figure 4: Mamiellophyceae genera contribution in SOLA environmental time series and microcosms. **A-** Seasonal patterns of reads assigned to Mamiellophyceae genera at SOLA. Note that only the two most abundant genera *Micromonas* and *Bathycoccus* can be seen on the graph. Grey dots correspond to the sampling dates of sea water for microcosms experiments. **B-** Barplot representing the number of reads per Mamiellophyceae genera in 4 microcosm experiments and their associated natural sample. Colors in the barplot refer to Mamiellophyceae genera, colors in the legend correspond to the month, when the initial sea water was sample and letters (in grey) to the incubation conditions (i.e. artificial month): March (M), June (J), September (S) and December (D).